DESIGN AND CONSTRUCTION OF A SIX DEGREE OF FREEDOM PLATFORM

A THESIS SUBMITTED TO
THE GRADUATE SCHOOL OF NATURAL AND APPLIED SCIENCES
OF
MIDDLE EAST TECHNICAL UNIVERSITY

BY

SARPER GÜRBÜZ

IN PARTIAL FULFILLMENT OF THE REQUIREMENTS
FOR
THE DEGREE OF MASTER OF SCIENCE
IN
MECHANICAL ENGINEERING

NOVEMBER 2006

Approval of the Graduate School of Natural and Applied Sciences.

Prof. Dr. Canan ÖZGEN
Director

I certify that this thesis satisfies all the requirements as a thesis for the degree of Master of Science.

Prof. Dr. Kemal İDER
Head of Department

This is to certify that we have read this thesis and that in our opinion it is fully adequate, in scope and quality, as a thesis for the degree of Master of Science.

Prof. Dr. M. A. Sahir ARIKAN
Co-Supervisor

Prof. Dr. Tuna BALKAN
Supervisor

Examining Committee Members

Prof. Dr. Mustafa İlhan GÖKLER	(METU, ME)	
Prof. Dr. Tuna BALKAN	(METU, ME)	
Prof. Dr. M. A. Sahir ARIKAN	(METU, ME)	
Asst. Prof. Dr. Buğra KOKU	(METU, ME)	
Dr. Tolga DURSUN	(ASELSAN)	

I hereby declare that all information in this document has been obtained and presented in accordance with academic rules and ethical conduct. I also declare that, as required by these rules and conduct, I have fully cited and referenced all material and results that are not original to this work.

Name, Last name :

Signature :

ABSTRACT

DESIGN AND CONSTRUCTION OF A SIX DEGREE OF PLATFORM

Gürbüz, Sarper
M.S., Department of Mechanical Engineering
Supervisor: Prof. Dr. Tuna BALKAN
Co-Supervisor: Prof. Dr. M. A. Sahir ARIKAN

November 2006, 83 pages

In this thesis a six degree of freedom (DOF) parallel manipulator is designed, developed and simulated virtually. The platform, which is specified and focused on in this thesis, is the specific solution for the generating the required data to simulate a land, airborne or sea vehicle's motion trajectory in the laboratory environment.

After explaining the need for such platforms for the military industry, the existing devices will be presented and discussed. Then the design period will be explained while pointing out the key performance criteria. The gathered performance values of the first design iteration will be presented and the modifications done in order to get to the expected performance will be given. Finally an investigation, in order to find the maximum payload that the platform can handle, is performed and presented.

It is too hard to get to the desired performance values in mechanical design and manufacturing without using the CAD (Computer Aided Design) and CAM (Computer Aided Manufacturing) programs. In this thesis ProEngineer Wildfire® is used for solid modeling the components, the sub-assemblies and the final assembly, ANSYS Workbench® is used for investigating the modal behavior of the components, ADAMS® 2003 is used for the dynamic simulation of the mechanism, ADAMS/Flex®, ADAMS/AutoFlex® and ADAMS/Durability® are used to analyze the results when flexibility is embedded into the system. At the end of the thesis in Appendix section five technical drawings with the nominal dimensions are given in order to clarify the construction period. By the regulations that must be obeyed in ASELSAN only the nominal dimensions are given in the technical drawings. All the dimensional and geometrical tolerances are given in the approved technical drawings that are proprietary of ASELSAN.

Keywords: 6-Axis Motion Platform, Application of CAD and analysis programs, Electromechanical Design, Stewart Platform

ÖZ

ALTI SERBESTLİK DERECELİ, PARALEL BAĞLI EYLEYİCİLERDEN OLUŞAN PLATFORMUN TASARIMI VE OLUŞTURULMASI

Gürbüz, Sarper
Y. Lisans, Makina Mühendisliği Bölümü
Tez Danışmanı: Prof. Dr. Tuna BALKAN
Tez Yardımcı Danışmanı: Prof. Dr. M. A. Sahir Arıkan

Kasım 2006, 83 sayfa

Bu tezde altı serbestlik dereceli paralel bağlı eyleyicilerden oluşan bir platform tasarlanmış, geliştirilmiş ve sanal ortamda benzetimi yapılmıştır. Teze konu olan cihaz kara, hava ve deniz araçlarının hareket profillerini laboratuar ortamında gerçekleştirme özelliğini sağlamaktadır.

Askeri endüstrinin bu platformlara duyduğu gereksinim nedeni açıklandıktan sonra, hareket profili gerçekleştirme kabiliyetine sahip mevcut sistemler tanıtılacaktır. Daha sonra mekanik tasarım süreci kilit performans kriterlerine vurgu yapılarak anlatılacaktır. İlk tasarım süreci sonunda elde edilen performans değerleri sunulacak ve istenen performans değerlerine erişmek için yapılan değişiklikler anlatılacaktır. Son olarak platformun taşıyabileceği maksimum yük araştırılması sunulacaktır.

Günümüz teknolojisinin geldiği noktada, askeri endüstrinin istediği performans değerlerini çok kısa sürede ve az sayıda iterasyonla yakalamak mümkün olmaktadır. Bu da mekanik tasarım sürecinde CAD (Bilgisayar Destekli Tasarım) ve CAM (Bilgisayar Destekli İmalat) programlarının kullanılmasını kaçınılmaz kılmaktadır. Bu tezde platformu oluşturan alt parçaların katı modellerinin oluşturulmasında ProEngineer Wildfire®, bu parçaların modal davranışlarını incelemek için ANSYS Workbench®, katı modeli oluşturulan ve parçalarının modal davranışları performans kriterleriyle örtüşen platformun bilgisayar ortamında dinamik benzetiminin yapılmasında ise ADAMS® 2003 kullanılmıştır. Platformu oluşturan ve yapısal olarak kritik olan parçaları esnek olarak analiz edebilmek için ADAMS/Flex®, ADAMS/AutoFlex® ve ADAMS/Durability® yazılımları kullanılmıştır. Tezin sonunda platformun imalatı sırasında kullanılan bazı teknik resimlerin basitleştirimiş halleri verilmiştir. Bu resimlerin imalat konusunda fikir vereceği düşünülmektedir. Üretim sırasında kullanılan teknik resimler ASELSAN malı olup, ASELSAN prosedürleri gereğince tezde verilmesi yasaktır. Tezde verilen resimler üzerinde sadece temel ölçüler gösterilmiştir.

Anahtar Kelimeler: 6 eksen hareket benzetim platformu, CAD ve analiz programlarının mekanik tasarım süreci içinde uygulamaları, Elektromekanik tasarım, Stewart Platform

to whom whoever thought good things about me...

ACKNOWLEDGEMENT

I would like to thank to my supervisors Prof. Dr. Tuna BALKAN and Prof. Dr. M. A. Sahir ARIKAN for their support and for giving me endless motivation throughout this study. I am also grateful to Land Systems Design Unit of MGEO of ASELSAN for giving me the opportunity to make this study.

I would like to express my greatest thanks to Mr. M. Türker KARAYUMAK (Mech. Eng., MSc.) and Mr. Serhat BAŞARAN (Aerospace Eng.) for their brotherhood, and Mr. S. Taylan TATAR (Mech. Eng.) for his neighborhood.

Finally I would like to send my deepest feelings to mom, dad and my brother who are always together with me no matter how far.

TABLE OF CONTENTS

LIST OF TABLES

LIST OF FIGURES

CHAPTER 1

INTRODUCTION

ASELSAN Inc., which has a great influence in guiding the national military defense sector, signed a contract with the Turkish Armed Forces in 2001 that is "The Modernization of 165 Leopard 1A1/1A4 Main Battle Tanks". The most important aspect of the project is embedding a fire control system into the main battle tanks. In order to obtain a perfect fire control on the main battle tanks, a gyroscopically stabilized 2-axis head mirror is designed and manufactured. The main function of this electromechanical system is to overcome the disturbances that are encountered by the tank and hold itself stabilized around the desired position in order to give the gunner a stationary scene in every operating condition and in every terrain. Meanwhile the designers of the Land Systems Design Unit of MGEO Division of ASELSAN has decided to build a testing platform for this electromechanical system since it would be very hard to test the performance after each mechanical and electronic modification in the field under actual operating conditions. This platform should be able to create the disturbances as the tank encounters during its mission. Thus the project of "Design and Manufacturing of a Six Degree of Freedom Platform" has been started which is the title of this thesis.

In this chapter, a brief description of main battle tanks and the motion trajectories that they usually encounter during operation is given. Different kinds of motion simulating devices are stated and the principal ideas behind the designs are considered. Then the need for such a platform in military industry will be discussed. The tools that are used in the preparation of the thesis are described and finally the scope of this study will be presented.

1.1 Brief Description of Main Battle Tanks

Main battle tanks are the core fighting vehicles aiming to destroy either stationary or moving targets.

Figure 1.1 Main Components of a Main Battle Tank

Battle tanks are the core fighting vehicles aiming to destroy either stationary or moving targets. Figure 1.1 shows the main components of a main battle tank. They are considered mainly in two sections. The first one is the turret which has 360xn degrees rotation capability with respect to the hull. The barrel and all the fire control equipment (gunner's sight, commander's sight etc.) are equipped on the turret. The barrel also has a degree of freedom with respect to the turret that is usually minimum -10 degrees and maximum +22 degrees measured from the level position. The other section is the hull which has all the power generation units, transmission and the palettes. It gives mobility to the main battle tank. The main battle tanks are the most popular fighting vehicles of the land forces of the national armies.

There exists a common terminology in order to describe the motion trajectory of the dynamic systems. If it is applied to the main battle tank it can be shown like this in Figure 1.2.

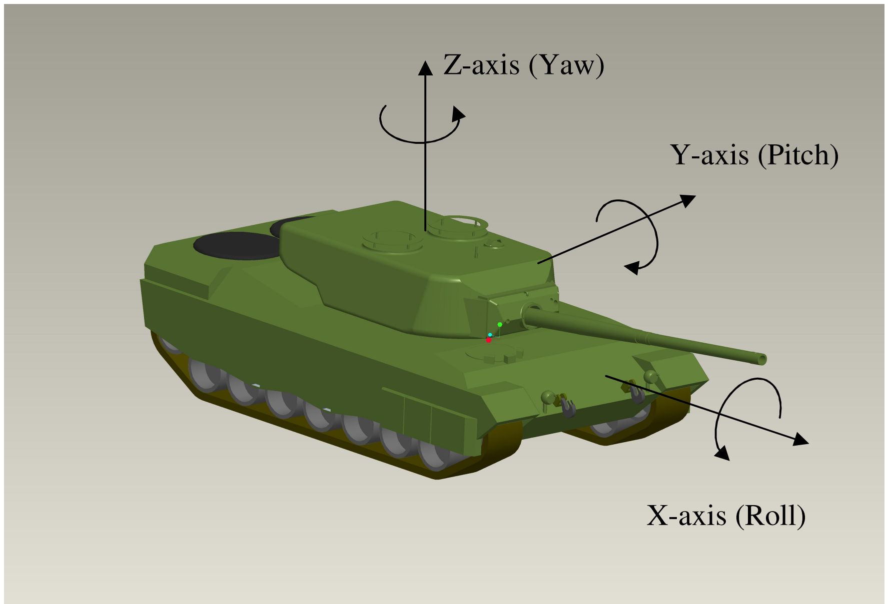

Figure 1.2 Motion Terminology of a Main Battle Tank shown on the solid model of a Leopard 1A3 tank

The motion characteristics imply on six different directions. These are three rotational and three linear directions. The linear velocity direction of the tank is called x-axis and the rotational motion around this axis is called roll motion. The direction which is on the same horizontal plane and perpendicular to x-axis is called y-axis and the rotational motion around this axis is called pitch motion. Eventually the third linear direction which is mutually perpendicular to the other two axes is called z-axis and the motion around this axis is called yaw motion. It is important to define the motion directions clearly in order to express the tank motion neatly.

Performance tests of the main battle tanks are usually performed on a special track called APG (Aberdeen Proving Ground) on which different barriers with different heights are placed at different positions. These heights and positions are predetermined by military standards. During these tests three rotational velocities and three rotational accelerations are recorded via gyroscopes and accelerometers respectively. Figure 1.3 shows an example pitch data collected in the field. These data will be sufficient to describe the land vehicle's motion on the move. Therefore in order to test the equipment that is integrated on the tank the designers either go to the field and create the operating conditions every time or the designers collect the tank's motion data once on the field and evaluate the collected motion data and perform this data on a platform in the laboratory environment. As it can be seen from the number and types of motion there should be platform that is capable of creating the disturbances in six individual axes in order to simulate the main battle tank's motion. Also, it should be controllable to manipulate the data.

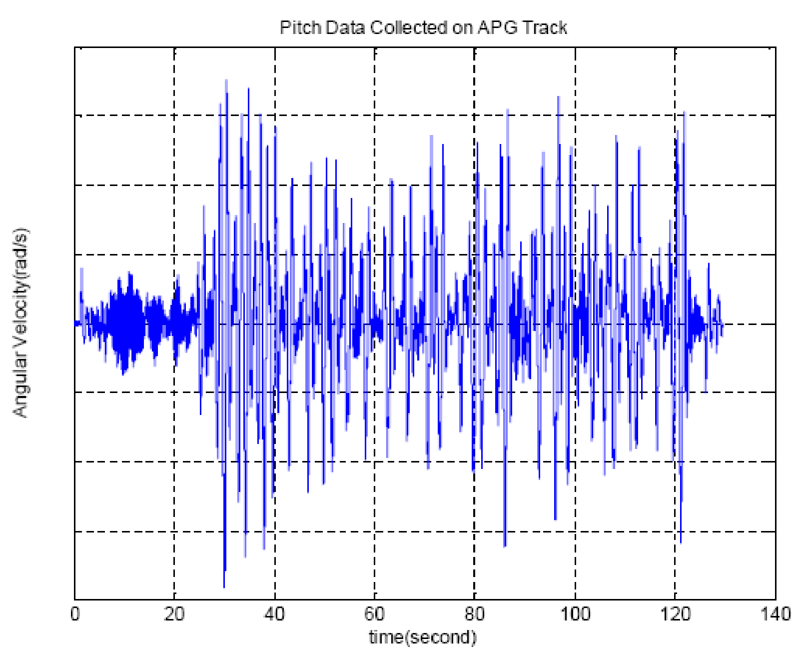

Figure 1.3 Gyroscope data in pitch direction collected in the field

1.2 Motion Simulating Devices

Simulators are mainly used for testing, entertainment and educational purposes. The complexity and the cost of the simulator increases as the degrees of freedom that the simulator can perform increase. In ASELSAN facilities a two axes motion simulator has been designed and constructed in order to test the turret alone in pitch and yaw directions in the laboratory environment. Figure 1.4 shows the two axis motion simulator.

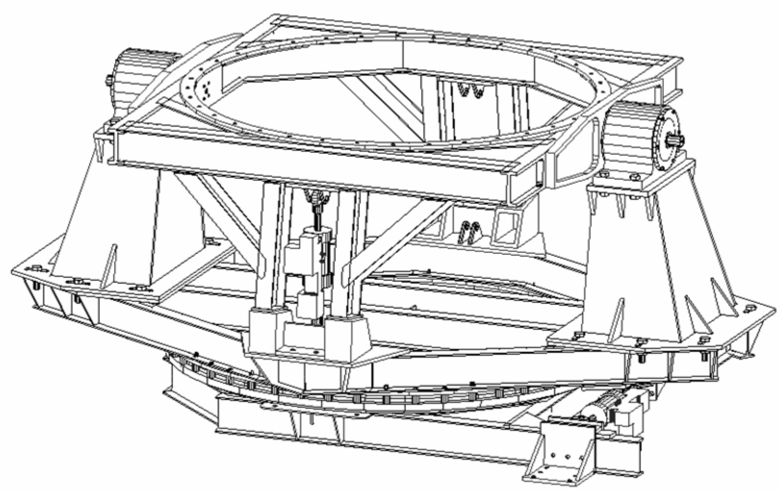

Figure 1.4 Two axis motion simulator of ASELSAN for testing the stabilization performance of the turret

This two axis simulator is a gimbal design that is formed from elevation and azimuth axes. The turret is mounted on the top plate on the elevation axis and the azimuth axis carries all the mechanics. This is a very good example of motion simulation in two axes since it is not too complex but enough to simulate the turret dynamics. The gimbal design also allows the simulator to perform both motions simultaneously.

The idea for motion simulation in six axes is first appeared with the increasing need for aircraft simulators. In order to test the aircraft performance, the designers looked for alternatives to create the flight conditions in the laboratory environment. In order to have all degrees of freedom of the spatial space a six axes simulator is needed as in the case of the main battle tank on the field. The first one these simulators is designed by Stewart and Gough in 1965. Then the name of "Stewart Platform" has been given to the six axis manipulators while honoring its inventor. Stewart Platform is a parallel kinematic machine that is found by struts and joints. Figure 1.5 shows an example for a parallel kinematic machine.

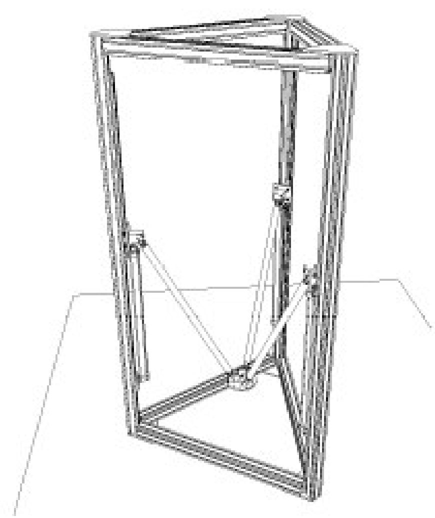

Figure 1.5 Three degree of freedom parallel kinematic machine

Parallel kinematic machines have its own actuators connected in a parallel manner that means the payload is shared nearly equally between the actuators. This is very advantageous in high payload applications in terms of single actuator load carrying capacity.

Parallel kinematic machines perform interesting performances compared to serial kinematic machines under several aspects. Thus the industrial interest for these machines is increasingly growing. Stewart Platform is a parallel kinematic machine that satisfies the requirements for motion simulation. The most important priority of the parallel kinematic machines over serial kinematic machines is less actuator effort since the payload is distributed equally over the actuators. However, there exists a drawback in terms of controllability. Controlling parallel kinematic machines is much more complicated than controlling serial kinematic machines.

Stewart Platforms are widely used not only for military applications but also for entertainment, manufacturing and medical applications. Six degree of freedom entertainment supported with graphical interfaces is nearly simulating reality. (Figure 1.6)

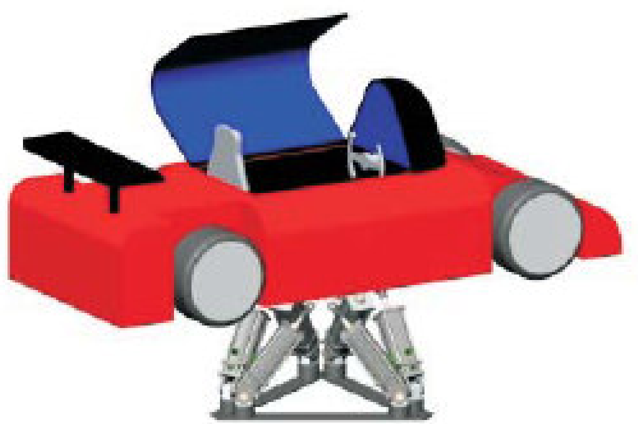

Figure 1.6 Stewart Platform as an entertainer

1.3 Military Applications

One of the core examples for military applications for Stewart Platform is to simulate the aircraft motion and train the pilot in the real combat environment. The most important aircraft simulation platform in Türkiye is used by the Turkish Air Forces, which has been developed by Havelsan.

Figure 1.7 Havelsan CN 235 Simulator

Havelsan CN 235 Simulator is designed and constructed abroad and all the mechanics is bought from international companies whereas the implementation of the software is done by Turkish engineers. This simulator is designed to simulate the real fighting conditions while saving expensive fuel and expenditure. One other advantage for the simulator is overwhelming the direct expenses for the maintenance that occurs from the training flight duration. The training can be done without taking care of the weather conditions, time and the planning of the other flights.

The CN 235 simulator has the following;

1. Real cockpit unit,
2. Sound simulation system,
3. Main computer unit,
4. Trainer console and trainer software,
5. VME bus data transfer,
6. Visualization screen,
7. Digitally controlled load sensation system,
8. 6 degree of freedom motion simulation system,
9. Air radar simulation system,
10. Power distribution system,
11. Debriefing system,
12. Security and emergency systems.

The other example for the military applications of Stewart Platform is the subject of this thesis. Stewart Platform (Figure 1.8) is designed and constructed in ASELSAN facilities for simulating the motion of the main battle tanks and observe the performances of the electromechanical equipment that is integrated on the tank. Firstly dynamic modeling will be discussed. It will primarily focus on the electromechanical design of the platform by using the CAD software. The solid modeling of each component and the assembly will be explained in detail. Modal analysis of the main components is described and the results are discussed. The dynamic motion simulation of the platform in the virtual environment is explained and the results are discussed. After completing the prototype phase and building the platform the needs had been modified and the design has to be modified. This iteration process will be explained, the modifications are told and the final performance will be discussed. Finally the maximum payload investigation that the platform can handle is explained. In the Appendix section five technical drawings from the manufacturing period, three of them showing the platform outline dimensions and two of them showing the top frame and the base, are given.

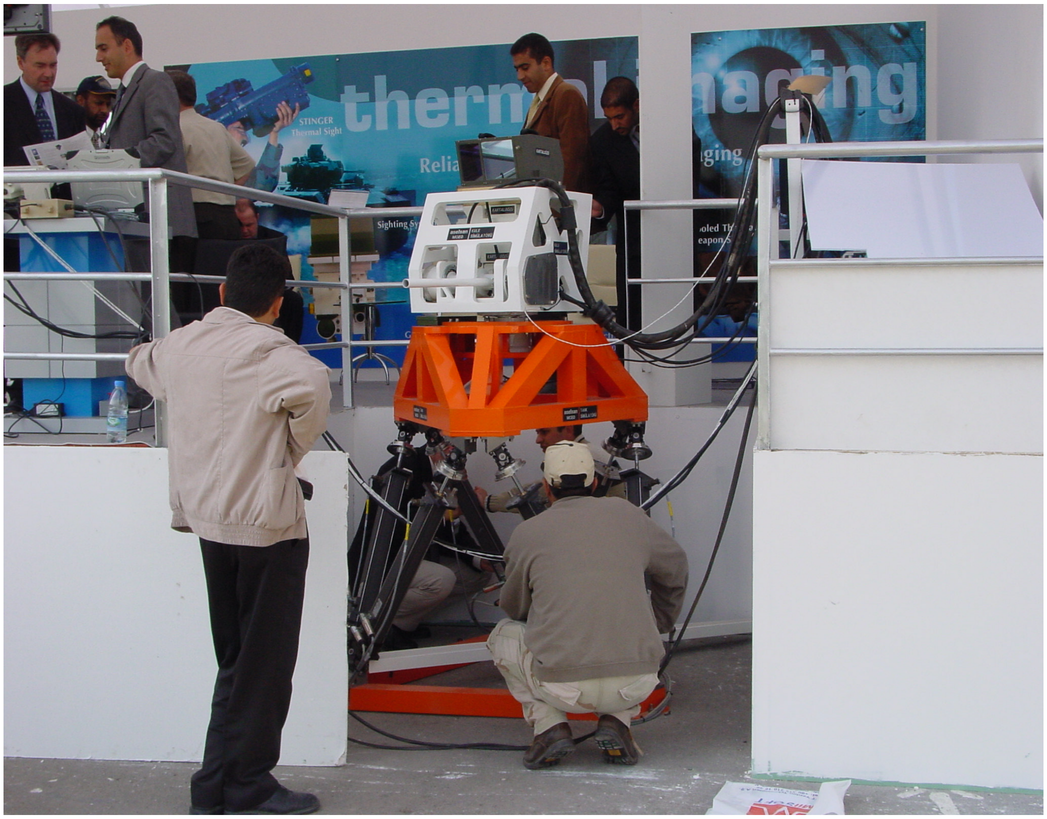

Figure 1.8 ASELSAN 6-DOF motion simulator on air in IDEF2003

The main purpose of this thesis is to design and construct a testing platform for ASELSAN. The product has been designed and produced and is actively used.

This thesis implies the electromechanical design of the Stewart Platform. The design and implementation of the closed loop control of the system is held in a cooperative study with Mr. Onur ALBAYRAK (Mech. Eng., MSc.) in ASELSAN. This study is also prepared and presented as a thesis named ‘Modeling and Real-Time Control System Implementation for a Stewart Platform’ in METU.

After producing the platform and demonstrating it in IDEF2003, it has attracted too many engineers in the defense sector. This thesis will be a perfect guide for the people who are interested in designing multi degree of freedom platforms.

The electromechanical design period which is explained in detail in this thesis is described briefly as a flowchart in Figure 1.9. This flowchart gives an intuition about the design period and clarifies the idea of using CAD programs during the design period of the Stewart Platform.

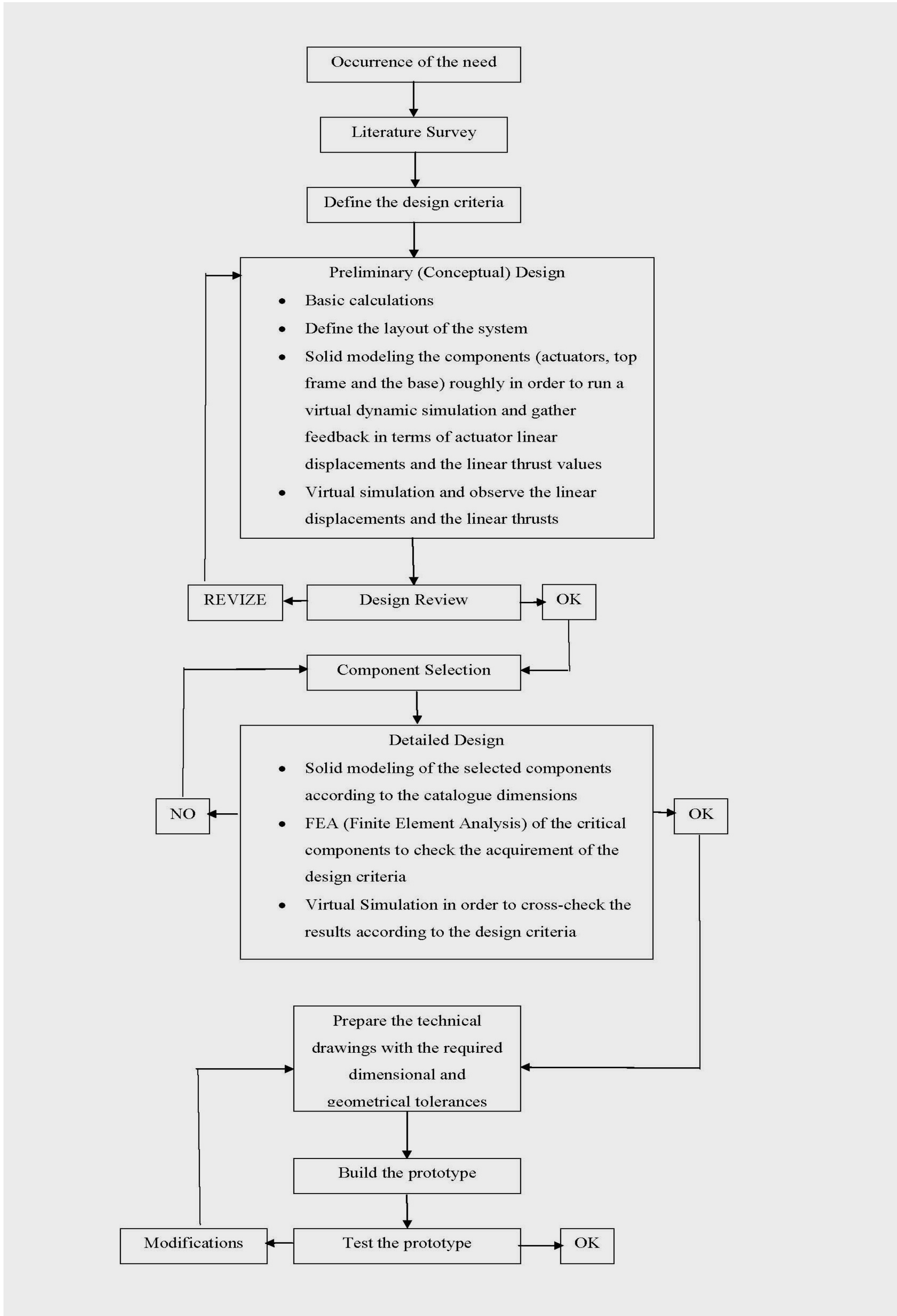

Figure 1.9 Design Flowchart

CHAPTER 2

ELECTROMECHANICAL DESIGN USING CAD FACILITIES

In this chapter electromechanical design of the platform using CAD software is considered. Firstly the predefined design criteria of the final equipment are explained. Secondly the components of the system are described and the solid models that are produced in ProENGINEER Wildfire® 2.0 are given with the technical specifications. Thirdly the modal analyses of the critical components that are obtained via ANSYS Workbench® are presented. Finally the dynamic simulation of the virtual prototype is given which is handled with ADAMS® 2003.

2.1 Design Criteria

In every mechanical design before starting everything the design criteria should be neatly specified since the component selection and the preliminary design phase strongly needs certain values to rely on. The most important design criteria throughout the design of the platform are the working space that directly affects the stroke of the linear actuators, rigidity that directly affects the controllability of the system, and the payload that directly affects the linear thrust that should be given by the linear actuators.

Working Space: The working space of the platform has to be capable enough to perform the defined motion that represents the main battle tank moving on the terrain. This motion can be identified via sensors mounted on the tank. The estimated values according to the measurements are given underneath in Figures 2.1 and 2.2.

Signal:	1	2	3	4	5	6	7	8
Frequency (Hz):	1	2,5	5	10	17	23	30	40
Magnitude (rad/s):	0.238	0.028	0.0084	0.0042	0.0123	0.045	0.021	0.0028

Figure 2.1 Recorded motion values in elevation axis

These values are also used in the azimuth axis. These are the main disturbance components that can be superimposed to define the motion of the tank in the working environment. The working space of the platform should be able to perform the motion that is formed by the superposition of these disturbance signals that can simulate the tank motion on the terrain with the linear frequency and magnitude.

Signal:	1	2	3	4
Frequency (Hz):	1	2,5	5	10
Magnitude (rad/s):	0,338	0,025	0,009	0,004

Figure 2.2 Recorded motion values in azimuth axis

Rigidity: The system should be as rigid as possible in order to increase controllability that is; increasing the frequency spectrum that the output can follow the input both in terms of magnitude and phase. In order to obtain this the mechanical design should be verified carefully before the manufacturing process starts. This verification has been done using ANSYS Workbench®. The modeled components have imported into the finite element solver and the design is reviewed according to the output results. The system should be as rigid as possible up to the frequencies of 120 Hz which is the design criteria in terms of rigidity coming from the modal characteristics of the testing equipment and the field data collected on the field.

If the components' flexible modes fail to lie in the specified range of frequency spectrum the necessary modifications should be performed.

Payload: The linear actuators of the platform should be capable of giving the necessary linear thrust to cope with the payload of the testing equipment which is 120 kg. The individual payload of each component will be explained later.

2.2 Solid Modeling Using ProEngineer Wildfire® 2.0

Virtual prototyping is a very common way that is used by the designers in the defense industry. It decreases the cost while increasing the quality and the durability of the products. When the models of the components are prepared the system can be tested and iterated without producing the final product. The modeled components are given underneath.

2.2.1 The Base

The base is the part that lies on the lowermost region of the assembly. It carries all the equipment and fixed to the ground by six M12 (metric) screws. The wedges that carry the universal joint assemblies are connected to the base on the three edges with four M10 screws. The wedge carriers are produced from Aluminum 6061 and coated with hard anodizing which increases the rigidity without increasing the total weight. The columns are Aluminum profiles with 80X80X2.5 mm dimensions. They have 45° faces in order to have flat welding surfaces on the mating part with the wedge carriers. The wedge carriers are welded to the profiles on twenty four edges of six faces. The base must be both rigid and lightweight. It must be rigid since it is the skeleton of the assembly and lightweight because the system must be transferable. The geometry is a equilateral triangle. Aluminum profiled columns and the wedge carriers are shown in detail in Figure 2.3.

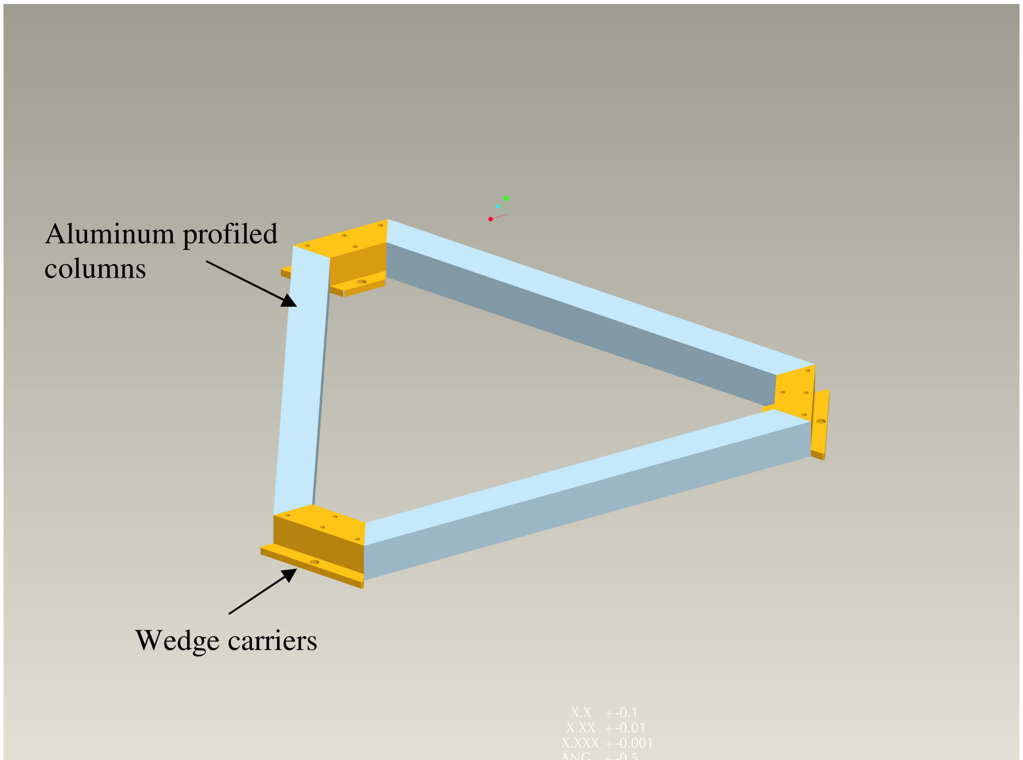

Figure 2.3 The Base

2.2.2 The Wedges

The wedges are the connecting parts between the base and the universal joint assemblies. Each wedge carries two universal joint assemblies. The wedge and the universal joint assembly are connected with four M8 screws. The wedge has two universal joint connection faces which have two orientation angles in order to obtain the initial configuration of the system. This orientation is obtained by iterations using MATLAB/Simmechanics® and it relaxes the actuators on the statically resting position with respect to the load carrying capacity. The two angled faces also determine the initial configuration and prevent the collision and interference. The general view of the wedge is shown in Figure 2.4.

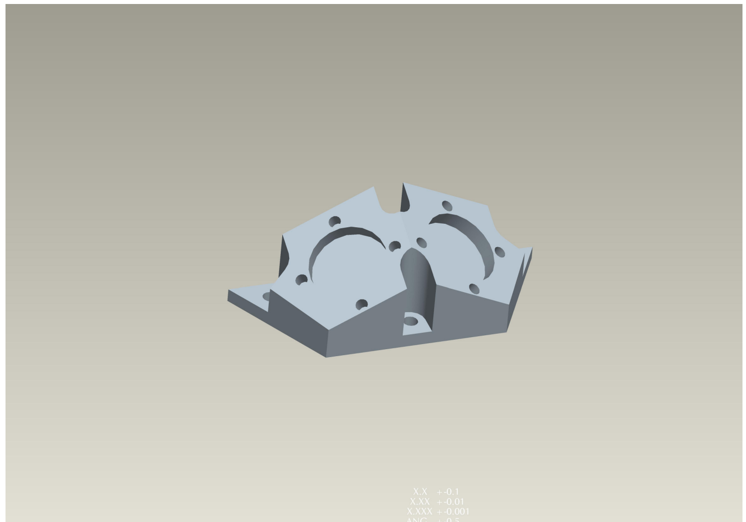

Figure 2.4 The Wedge

The two individual face angles are shown in terms of back view and side view of the wedge. Figures 2.5 and 2.6 show different views of the wedge.

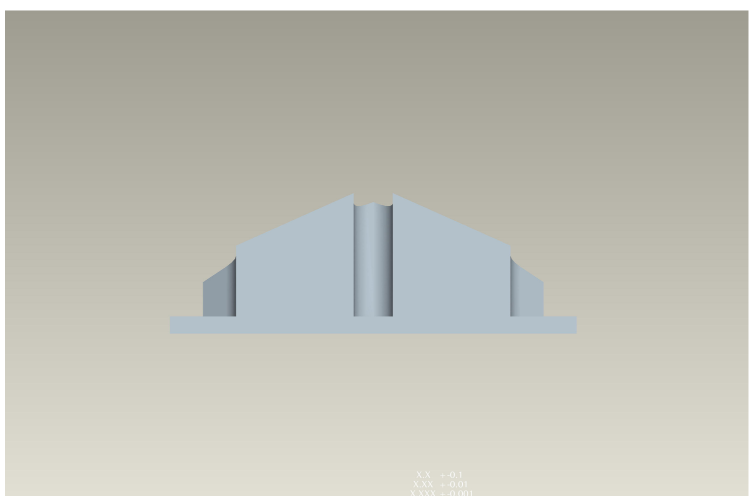

Figure 2.5 The wedge from the back showing the first face angle

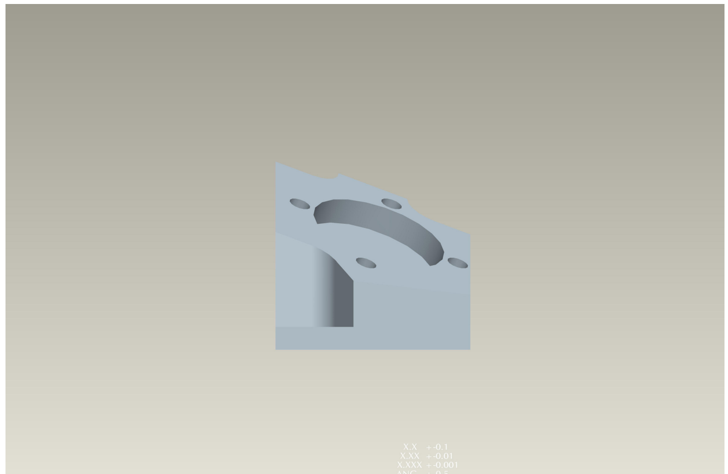

Figure 2.6 The wedge from the left showing the second face angle

When the wedges are assembled to the base on the three edges the system becomes ready for assembling universal joint assemblies as shown in Figure 2.7.

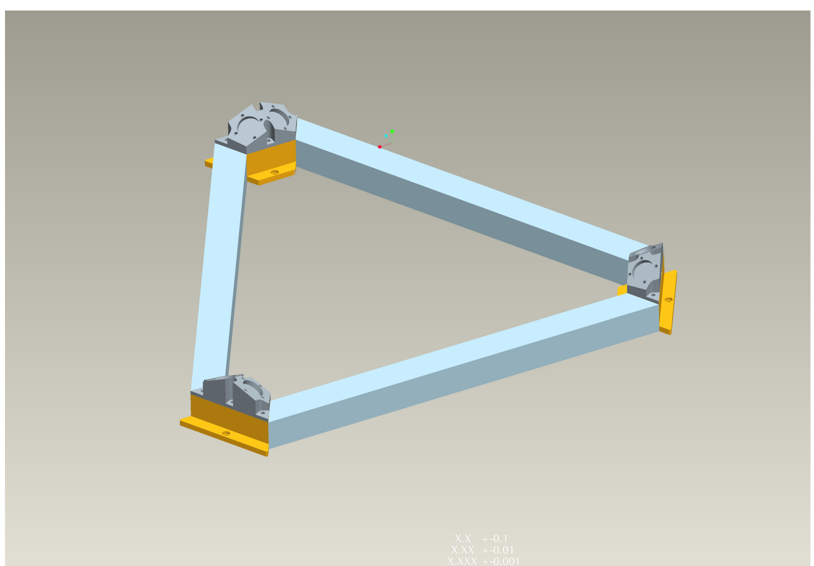

Figure 2.7 Wedges assembled on the base

2.2.3 The Universal Joints

When considering the joints used in an electromechanical robotic system there are several important aspects that have to been taken into consideration. Firstly the degree of freedom of the joint is important. When deciding the numbers of degrees of freedom of the joints the Grübler's Equation is benefited. The equation is as follows;

$$DOF= \lambda * (L-j-1) + \Sigma f_i$$

where $\lambda = 3$ for planar

$\lambda = 6$ for spatial cases,

L = # of the links,

j = # of the joints,

f_i = allowable degree of freedom of each joint.

When Stewart Platform is considered;

L= 1 (ground frame) + 1 (top frame) + 6 (housings of the linear actuators) + 6 (shafts of the linear actuators) = 14

j = 6 (ground universal) + 6 (prismatic) + 6 (top spherical) = 18

$$\mathbf{DOF = 6* (14\text{-}18\text{-}1) + 6*2 + 6*1 + 6*3 = 6}$$

As it can be seen from the equation if linear actuators are used 6 prismatic joints are guaranteed. The ground and top joints can be set either universal or spherical joints. In ASELSAN motion simulator ground joints are set as universal joints. Secondly the stiffness, friction and the backlash of the joint is critical. In order to accommodate this criteria needle bearing universal joints of the BELDEN Inc. in USA are selected.

Needle bearing universal joints are fitted with high quality, pre-lubricated and double O-ring sealed needle bearings to provide precise positioning and continuous operation at speeds up to 5,000 rpm. Needle bearing universal joint is even stronger and longer lasting than its counterpart and has the capability to be rebuilt when wear and tear occurs. Needle bearing universal joints are designed to maintain low backlash for the critical positioning applications required by robotics, shift linkage, and instrumentation. Additionally, needle bearing universal joints are excellent for continuous operation applications. Figure 2.8 shows the exploded view of the joints.

The technical specifications of the needle bearing universal joints are as follows;

- Operation at high RPM
- Near zero backlash
- Continuous operation
- Operating angles up to 35°
- Rigid axial stiffness for push/pull loads

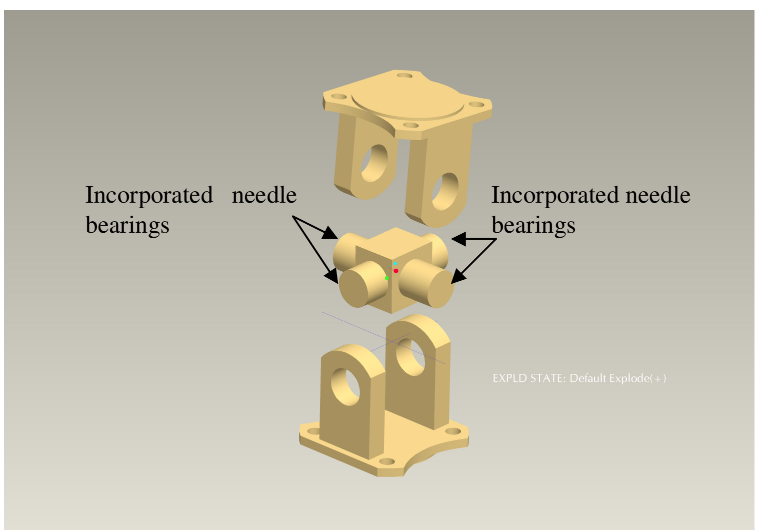

Figure 2.8 Exploded view of the needle bearing universal joint assembly

The real picture of the needle bearing universal joint assembly is shown in Figure 2.9;

Figure 2.9 Belden Inc. needle bearing universal joint assembly

Catalogue specification of the BELDEN Universal Joint is shown in Figure 2.10.

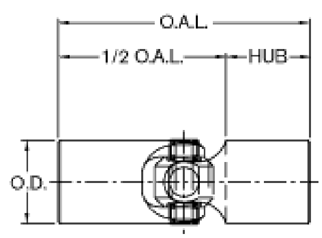

Part No.	O.D.	OAL	1/2 OAL	HUB PROJ.
UJ-NB750	0.25 inch	2.7 inch	1.35 inch	0.93 inch
UJ-NB1000	1 inch	3.375 inch	1.7 inch	1.2 inch
UJ-NB1250	1.25 inch	3.75 inch	1.875 inch	1.25 inch
UJ-NB1500	1.5 inch	4.25 inch	2.125 inch	1.375 inch
UJ-NB40	40 mm	5.5 inch	2.25 inch	2 inch

Figure 2.10 BELDEN Inc. needle bearing universal joint catalogue

Another alternative for the universal joint is the CURTIS Universal Joints from USA. The schematic picture of the alternative universal joint is given in Figure 2.11.

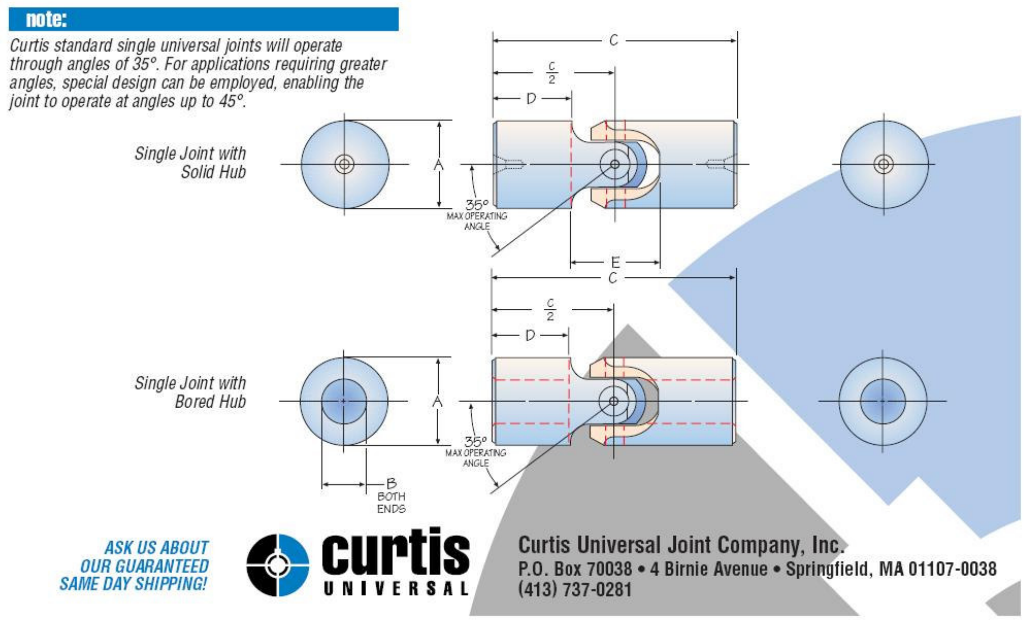

Figure 2.11 Schematic picture of the Curtis Universal Joint

When the catalogue values of the alternative is examined it can be seen that the alternative can easily be replaced with the selected universal joint. But in every component selection phase of a design period one important concept arises which is the cost comparison of the components. The BELDEN Universal Joint is appeared much more cost effective than the CURTIS Universal Joint when the quotations are presented by the companies. So the BELDEN Universal Joint is selected to use in the Stewart Platform.

Figure 2.12 shows the catalogue values of the CURTIS Universal Joint.

SELECTION GUIDE - ALLOY STEEL
BLOCK AND PIN TYPE STANDARD SINGLE JOINTS
MEET MILITARY SPEC. MIL-U-20625A, CLASS A

SINGLE JOINTS		BREAKING LOADS		DIMENSIONS OF STANDARD JOINTS IN INCHES					APPROXIMATE WEIGHT IN POUNDS	
Standard Solid Hub	Standard Bored Hubs Bore 1/2 of O.D.	Static Torque Rating	Compression or Tension Load	Outside Dia. "A"	Bore Dia. "B"	Total Length "C"	Hub/Bore Length "D"	Shaft to Shaft Distance "E"		
Cat. No.	Cat. No.	Inch Pounds	Pounds	+.000 -.003	±.001	±1/64 **±1/32	±1/64		Solid Hubs	Bored Hubs
CJ641	CJ641B	140	—	3/8'	3/16"	1-3/4'	11/16'	3/8"	.05	.04
CJ642	CJ642B	425	1200	1/2'	1/4'	2'	3/4'	1/2"	.10	.08
CJ643	CJ643B	900	2000	5/8'	5/16"	2-1/4'	13/16"	5/8'	.18	.14
CJ644	CJ644B	1610	3200	3/4'	3/8'	2-11/16'	31/32'	3/4"	.30	.24
CJ645	CJ645B	1800	4600	7/8'	7/16"	3'	1-1/32"	15/16"	.45	.31
CJ646	CJ646B	3050	5600	1'	1/2'	3-3/8'	1-3/16"	1"	.66	.50
CJ647	CJ647B	3500	6000	1-1/8'	9/16"	3-1/2'	1-7/32"	1"	.88	.69
CJ648	CJ648B	5500	8800	1-1/4'	5/8'	3-3/4'	1-1/4'	1-1/4"	1.15	.88
CJ650	CJ650B	9000	14000	1-1/2'	3/4'	4-1/4'	1-11/32'	1-9/16"	1.81	1.44
CJ651	CJ651B	14000	18000	1-3/4'	7/8'	**5'	1-9/16"	1-7/8"	2.86	2.31
CJ652	CJ652B	22000	25000	2'	1'	**5-7/16"	1-5/8'	2-3/16"	4.06	3.31
CJ653	CJ653B	32000	35000	2-1/2'	1-1/4'	**7'	2-3/32"	2-13/16"	8.25	6.81
CJ654	CJ654B	55000	—	3'	1-1/2'	**9'	2-27/32'	3-5/16"	15.25	12.5
CJ655	CJ655B	131000	—	4'	2'	**10-5/8"	3-1/8'	4-3/8"	31.3	25.8

Figure 2.12 Catalogue values of the CURTIS Universal Joint

2.2.4 The Custom Design Adapters between linear actuators and the universal joints

Since the universal joints and the linear actuators are gathered from different companies as well as the products are not produced based on special purpose an outcome for the need of an adapter has occurred. This adapter should have to maintain the connection between universal joints and the linear actuators. This part should be as rigid as possible and has the ability to be mounted on both parts easily. Adapter has been manufactured from a block of stainless steel and put into a black oxiding process. It has a channel to get out the cable of the linear variable differential transducer which is used to get the data of linear displacement of the linear actuator. Producing the part from block material increases the rigidity of the part whereas it increases the total weight which is not a critical concern when designing connector parts. Technical drawings of the part has been prepared and sent to the manufacturers of both needle bearing universal joint and the linear actuator. Both companies agreed on the design and the part has been manufactured. Figure 2.13 shows the adapters.

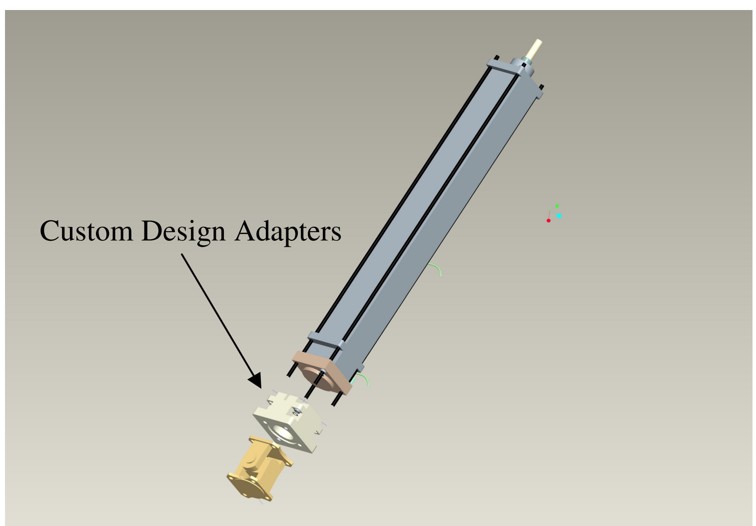

Figure 2.13 Custom Design Adapters between linear actuator and the universal joint

2.2.5 The Linear Actuators

The linear actuators occupy the most important part of the design. In the later parts of the thesis modal analysis of the actuators with or without the linear guides and the selection criteria of the actuators by using virtual dynamic simulation will be discussed. Hereby in 2.2.5 the working principle of the linear actuators and the solid model will be presented.

There are mainly five different types of linear actuators that are used in electronic positioning applications. These are ACME screw mechanism linear actuators, ball screw mechanism linear actuators, roller screw mechanism linear actuators, hydraulic cylinders and pneumatic cylinders. The comparison of five types is given on the table shown in Figure 2.14. The most important aspects for Stewart Platform are speed, acceleration, electronic positioning, stiffness and friction. If the table is examined it can be seen that roller screw mechanism linear actuators are the most suitable actuators that can be used for designing the motion platform.

	EXLAR ROLLER SCREWS	ACME SCREWS	BALL SCREWS	HYDRAULIC CYLINDERS	PNEUMATIC CYLINDERS
Load ratings	Very High	High	High	Very High	High
Lifetime	Very long, many times greater than ball screw	Very low, due to high friction & wear	Moderate	Can be long with proper maintenance	Can be long with proper maintenance
Speed	Very high	Low	Moderate	Moderate	Very high
Acceleration	Very high	Low	Moderate	Very high	Very high
Electronic Positioning	Easy	Moderate	Easy	Difficult	Very Difficult
Stiffness	Very high	Very high	Moderate	Very high	Very low
Shock Loads	Very high	Very high	Moderate	Very high	High
Relative Space Requirements	Minimum	Moderate	Moderate	High	High
Friction	Low	High	Low	High	Moderate
Efficiency	>90%	approx 40%	>90%	<50%	<50%
Installation	Compatible with standard servo electronic controls	User may have to engineer a motion/actuator interface	Compatible with standard servo electronic controls	Complex, requires servo-valves, high pressure plumbing, filtering, pumps linear positioning & sensing	Very complex requires servo-valves, plumbing, filtering, compressors linear positioning & sensing
Maintenance	Very low	High due to poor wear characteristics	Moderate	Very high	High
Environmental	Minimal	Minimal	Minimal	Hydraulic fluid leaks & disposal	High noise levels

Figure 2.14 Comparison Table

Roller Screw is a mechanism for converting rotary torque into linear motion in a similar manner to ACME screws or ball screws. Multiple threaded helical rollers are assembled in a planetary arrangement around a threaded shaft which converts a motor's rotary motion into linear movement of the shaft or the nut. The number of contact points in a ball screw is limited by the ball size. Roller screw designs provide many more contact points than possible on comparably sized ball screws. Since the number of contact points is greater roller screws have higher load carrying capacities, plus improved stiffness. Another advantage with their load carrying capacities roller screws deliver major advantages in working life. When higher loads and faster cycling is desired roller screws provide an attractive alternative to the hydraulic and pneumatic options. With their vastly simplified controls electromechanical units using roller screws have major advantages. They do not require a complex support system of valves, pumps, filters and sensors. Besides hydraulic fluid leaks are not existent, noise levels decrease dramatically and computer programmed positioning becomes very desirable.

For the listed reasons above EXLAR Company's (USA) GSX30-1802-MCA-ER1-238 -EB-AR-LT model linear actuator with roller screw mechanism is selected. Here GSX30-1802 stands for 457 mm stroke, 5.08 mm/rev lead linear actuator. M stands for connections of the cables (power, brake, resolver feedback...). These connections are done by interconnect military connectors. C stands for rear clevis mount at the back of the actuator and A for male metric threads M12 X 1.75 at the front of the actuator. ER1 stands for resolver feedback that can be used for precise positioning other than the linear variable transducer. 238 describes the motor characteristics; 2 stack, 230 V_{rms} and 8 pole motor is used for creating rotational motion. EB means 24 V electric brake can be used when the actuators are at rest or in case of any emergency. AR means anti-rotate option is used for guiding the shaft of the actuator so that linear motion is established. In order to explain this, roller screw mechanism linear actuator's working principle should be discussed. As it can be seen from Figure 2.15, 230 V_{rms} motor's stator is fixed at the back of the actuator to the housing.

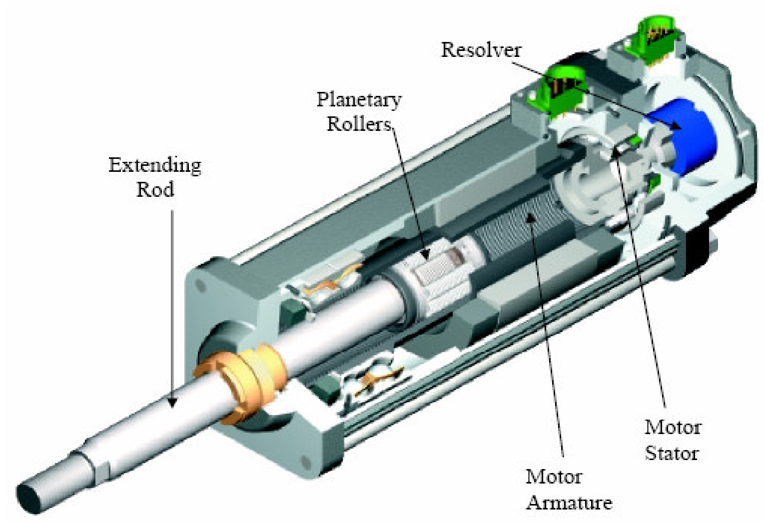

Figure 2.15 Sectional view showing the inside of the actuator

The extended rotor shown as motor armature has a hollow structure where it has a threaded inner section. The roller screws are put in a planetary manner over a cylindrical part. The extending rod is coupled to the planetary rollers and they form a single part. When the rotor has it motion from the stator, the rotor and the planetary rollers turn together. If the extending rod thus the planetary rollers are forced not to turn then the linear motion of the extended rod with respect to the housing is guaranteed. In order to have this motion EXLAR Company of USA has produced anti-rotate mechanism bars which are not used in this project due to stiffness reasons. In the later parts of the thesis linear guides that are designed by ASELSAN for having the linear motion will be explained. Figure 2.16 shows EXLAR's anti-rotate mechanism.

Since the platform will be used for testing military equipment the component selection is very important. All the manufacturer catalogues' are observed neatly and the performance price comparison is done. Best one is the EXLAR linear actuator.

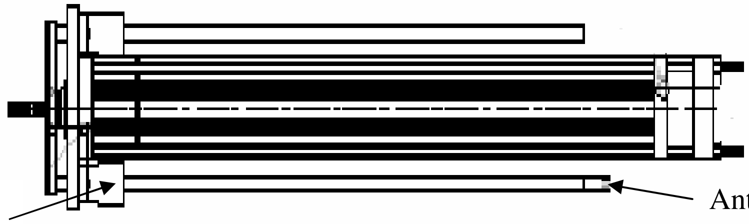

Figure 2.16 EXLAR's Anti-rotate mechanism

When the extended rod tends to rotate with respect to the housing the rods prevent the rotational motion with the help of the bushings. As mentioned above ASELSAN has designed its own anti-rotate mechanism, increased rigidity while decreased bushing friction dramatically which affects the closed loop control of the actuators majorly. The solid model of the linear actuator is prepared neatly according to the technical drawings received from EXLAR Company in order to take the precautions for preparing a perfect assembly. All the connection details are taken into consideration while the physical properties such as density is stated and the center of gravity and inertia terms of the solid model appeared as close as possible to the real linear actuator. The inertia values are described when explaining the virtual dynamic simulation of the platform with ADAMS® 2003. All six linear actuators mounted on the wedges without linear guides are shown in Figure 2.17.

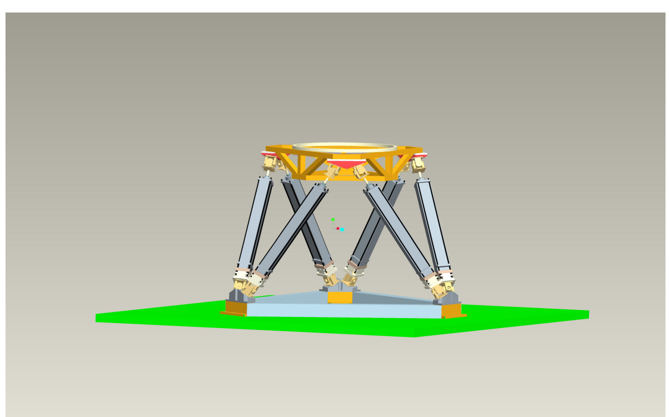

Figure 2.17 Stewart Platform without linear guides

The other alternatives for the linear actuators are PARKER (USA) and RACO (USA) companies other than the EXLAR company. The schematic picture and the catalogue values of the PARKER actuators are given in Figures 2.18 and 2.19 respectively.

Figure 2.18 PARKER linear actuator

Precision Actuators

		Type	Max travel [mm]	Max speed [m/s]	Max load [N]	Repeatability [μm]
LXR	CAD	Linear Motor Table	50…3000	3	950	±1
MX80	CAD	Screw Driven or Linear Motor	25…150	5	8	±0.4…5
LX80	CAD	Linear Motor	150…750	3	19…36	±1.5…2.5
XE	CAD	Economy Ballscrew Table	700	-	-	±20.0
XR	CAD	Ballscrew Table	50…2000	0.3…1.5	950	±1.3
XRS	CAD	Standard System	1000x1000	2.25	25	1
ZP	CAD	Vertical Lift "Wedge" Table	25	0.44	75	±3
RT	CAD	Rotary Tables	-	-	90	±12arc
LM	CAD	Screw Driven or Linear Motor	50 … 2000	3	6300	±2
Micro	CAD	Ballscrew Table	200	0.3	1150	±1
Ultra		Screw Driven or Linear Motor	500	1.5	18000	±0.5
RD	CAD	Direct Drive Rotary stage	-	-	-	4.1 arc-sec
HD	CAD	Linear Positioner (ballscrew)	1200…1600	1.48	-	±8

Figure 2.19 Catalogue values of the PARKER linear actuator

The schematic picture and the catalogue values of the RACO actuators are given in Figures 2.20 and 2.21 respectively.

RACO SCHWELM

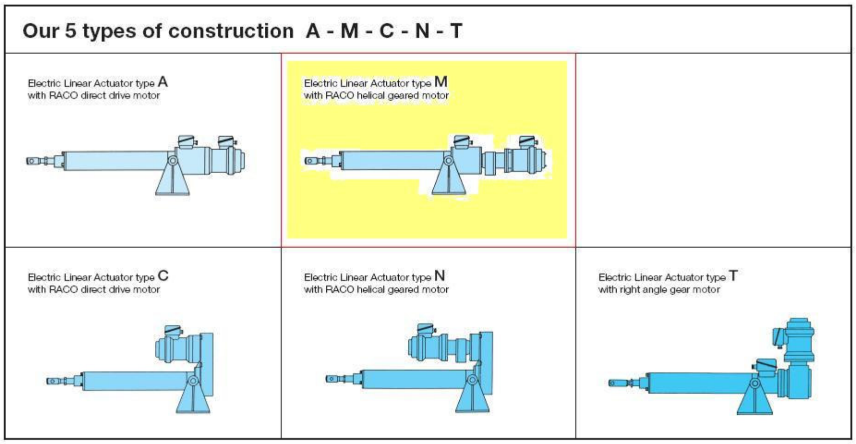

Figure 2.20 RACO linear actuator

TECHNICAL DATA AND DIMENSIONS FOR ELECTRIC LINEAR ACTUARORS — ACME SCREWS

Size	THRUST UNIT Stroke (mm)	a_3	Thrust (kN)	Speed (mm/s)	DRIVE MOTOR Type A a_5	Type A L**	Type A Motor size	Type M a_5	Type M L**	Type M Motor size	Type C a_{10}	Type C u_3	Type C Motor size	Type N a_{10}	Type N u_3	Type N Motor size	Type T a_5	Type T L	Type T L_1**	Type T Motor size
3	100	313	2,0	5				135	397	3				15	73	3	135	143	343	3
	200	413		10				135	397	3				15	73	3	135	143	343	3
	300	513		15				135	397	3				15	73	3	135	143	343	3
	400	613		20				135	397	3	15	73	3	15	73	3				
	500	713																		
	600	813	1,0	40	135	225	3				15	73	3							
	800	1013																		
	1000	1213																		
4	100	430	5,0	5				135	397	3				15	73	3	135	143	343	3
	200	530		10				135	397	3				15	73	3	135	143	343	3
	300	630		15				135	397	4				15	73	4	135	143	343	4
	400	730		30				135	397	4	15	73	4	15	73	4				
	500	830																		
	600	930	2,5	60	135	225	4				15	73	4							
	800	1130		120	135	225	4				15	73	4							
	1000	1330																		
5	100	455	10,0	5				135	397	3				18	116	3	135	143	343	3
	200	555		10				135	397	4				18	116	4	135	143	343	4
	300	655		15				135	397	4				18	116	4	135	143	343	4
	400	755		30				135	536	5	18	116	5	18	116	5				
	500	855																		
	600	955	5,0	80	150	285	5				18	116	5							
	800	1155		160*	150	285	5				18	116	5							
	1000	1355																		

Figure 2.21 Catalogue values of the RACO linear actuator

Finally the schematic picture and the catalogue values of the EXLAR actuator are given in Figures 2.22 and 2.23 respectively.

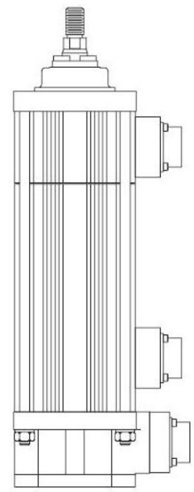

Figure 2.22 EXLAR linear actuator

GSX30 & GS30 Performance Specifications

Model	Frame Size in (mm)	Stroke in (mm)	Screw Lead in (mm)	Force* Rating lb (N) 1/2/3 stack	Max Velocity in/sec (mm/sec)	Continuous Motor Torque lb-in (N-m)	Maximum Static Load lb (N)	Armature Inertia lb-in-s^2 (Kg-m^2)	Dynamic Load Rating lb (N)	Weight (approx.) lb (Kg)
GSX30-0302	3.125 (79)	3 (76)	0.2 (5.08)	415/674/NA (1846/2998/NA)	10 (254)	16.5/26.8/NA (1.86/3.03/NA)	2000 (8896)	0.00319 (0.00036)	5800 (25798)	9.5 (4.3)
GSX30-0305	3.125 (79)	3 (76)	0.5 (12.7)	166/269/NA (738/1197/NA)	25 (635)	16.5/26.8/NA (1.86/3.03/NA)	2000 (8896)	0.00319 (0.00036)	4900 (21795)	9.5 (4.3)
GSX30-0602	3.125 (79)	5.9 (150)	0.2 (5.08)	415/674/905 (1846/2998/4026)	10 (254)	16.5/26.8/36 (1.86/3.03/4.07)	2000 (8896)	0.00361 (0.000408)	5800 (25798)	11.5 (5.2)
GSX30-0605	3.125 (79)	5.9 (150)	0.5 (12.7)	166/269/362 (738/1197/1610)	25 (635)	16.5/26.8/36 (1.86/3.03/4.07)	2000 (8896)	0.00361 (0.000408)	4900 (21795)	11.5 (5.2)
GSX30-1002	3.125 (79)	10 (254)	0.2 (5.08)	415/674/905 (1846/2998/4026)	10 (254)	16.5/26.8/36 (1.86/3.03/4.07)	2000 (8896)	0.00416 (0.00047)	5800 (25798)	19 (8.6)
GSX30-1005	3.125 (79)	10 (254)	0.5 (12.7)	166/269/362 (738/1197/1610)	25 (635)	16.5/26.8/36 (1.86/3.03/4.07)	2000 (8896)	0.00416 (0.00047)	4900 (21795)	19 (8.6)
GSX30-1402	3.125 (79)	14 (356)	0.2 (5.08)	415/674/905 (1846/2998/4026)	10 (254)	16.5/26.8/36 (1.86/3.03/4.07)	2000 (8896)	0.00473 (0.000534)	5800 (25798)	22 (10)
GSX30-1405	3.125 (79)	14 (356)	0.5 (12.7)	166/269/362 (738/1197/1610)	25 (635)	16.5/26.8/36 (1.86/3.03/4.07)	2000 (8896)	0.00473 (0.000534)	4900 (21795)	22 (10)
GSX30-1802	3.125 (79)	18 (457)	0.2 (5.08)	415/674/905 (1846/2998/4026)	10 (254)	16.5/26.8/36 (1.86/3.03/4.07)	2000 (8896)	0.00533 (0.000602)	5800 (25798)	25 (11.3)
GSX30-1805	3.125 (79)	18 (457)	0.5 (12.7)	166/269/362 (738/1197/1610)	25 (635)	16.5/26.8/36 (1.86/3.03/4.07)	2000 (8896)	0.00533 (0.000602)	4900 (21795)	25 (11.3)

Figure 2.23 Catalogue values of the EXLAR linear actuator

2.2.6 The Linear Guides with Linear Bearings

In order to establish linear motion within the actuators and have a more rigid configuration other than the EXLAR Company's anti-rotate mechanism new linear guides with SCHNEEBERGER Company's linear bearings are designed. The most important point here is each guide is supported with four linear bearings, two of them are placed on one side and the other two are placed perpendicularly to the other two linear bearings mounted surface of the linear actuator. Each actuator carries a fixed guide which is fixed from bottom to the custom design adapter and from top to the linear actuator's body. The carriages of the linear guides are fixed on the fixed guide. Besides each actuator carries a moving guide which carries the rails of the linear bearings. As mentioned above each linear bearing comprises of one rail and one carriage. In Stewart Platform two carriages support one rail thus one actuator has four carriages and two rails, all together it adds up to twenty four carriages and twelve rails. When choosing the linear bearings the considerations mentioned below are taken into account;

- High rigidity
- High static and dynamic load carrying capacity
- Good running smoothness in other words low friction
- Compact total enclosure

If the cases are examined respectively;

Rigidity: Linear guideways have significant effect on the overall rigidity of the system. The high rigidity of the SCHNEEBERGER is achieved by using rollers instead of balls as rolling elements and by the optimization of the cross section of the carriage and the rail. As it can be seen from the Figure 2.24 when the same load is applied on a ball with a roller, a ball is deformed more than the roller elastically. This means a roller is more rigid than a ball under the same loading conditions.

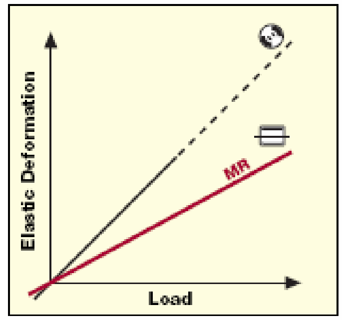

Figure 2.24 Elastic deformation vs. load of both ball and roller as rolling elements in a linear guideway

Load Carrying Capacity: In contrast to the circular arc ball guideway, the roller guideway has a flat and noticeably larger contact area. This results a substantially higher load carrying capacity and lower wear together with minimum rolling friction.

Running Smoothness: The running smoothness of the SCNEEBERGER roller guideways is the result of the optimized geometry of the roller tracks. As well as optimized geometry lubrication must be done periodically in case of optimum life. Minimized guideway travel pulsation and uniform translational force should be set in order to have low friction. This requires perfect assembly of the linear guideways on the linear actuators.

Compactness: The o-arrangement of the rollers causes force vectors to intersect outside, far from the rail center, allowing heavy loading by moments and forces in all directions. Also due to the geometric limitations the dimensional properties must be feasible and affordable. The o-arrangement of the rollers can be seen and understood more clearly in Figure 2.25.

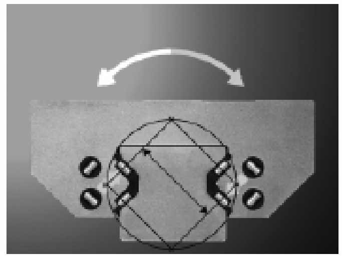

Figure 2.25 O-arrangement of the rollers which cause the cancellation of the forces acting in x-direction causing the elimination of unnecessary moments

According to the reasons considered above SCHNEEBERGER Company’s MRA 25 product has been selected. Dimensional properties and load carrying capacities of the product are shown in Figure 2.26.

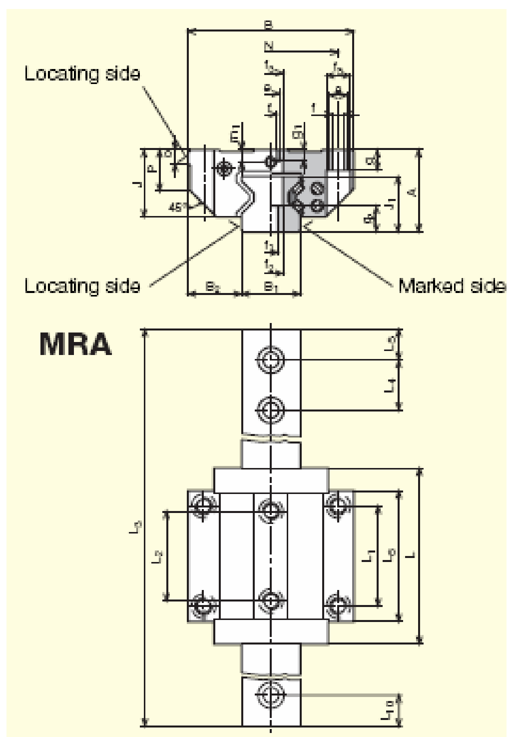

Figure 2.26 Dimensional clarification of the linear bearing

Type	Dimensions (mm) A	B	B_1 ±0.05	B_2	J	J_1	L	L_1	L_2	L_4	L_5/ L_{10}	L_6	N	e	f	f_1	f_2	f_3	Roller Ø	g	g_1	g_2	m_1	o	P
MRA 25	36	70	23	23.5	29.5	24.5	81	45	40	30	14	60	57	M 8	6.8	7	11	11	3.2	9	6.5	13	5.5	7.5	17.5

Loading capacities C_0 (N)	C (N)	Moments M_{0Q} (Nm)	M_{0L} (Nm)	M_Q (Nm)	M_L (Nm)	Weights Carriage (kg)	Rail (kg/m)
49 800	27 700	733	476	408	265	0.7	3.4

Figure 2.26 cont'd

The solid model of one linear guideway and the subassembly of the guideways and the linear actuator are shown below in Figures 2.27 and 2.28 respectively;

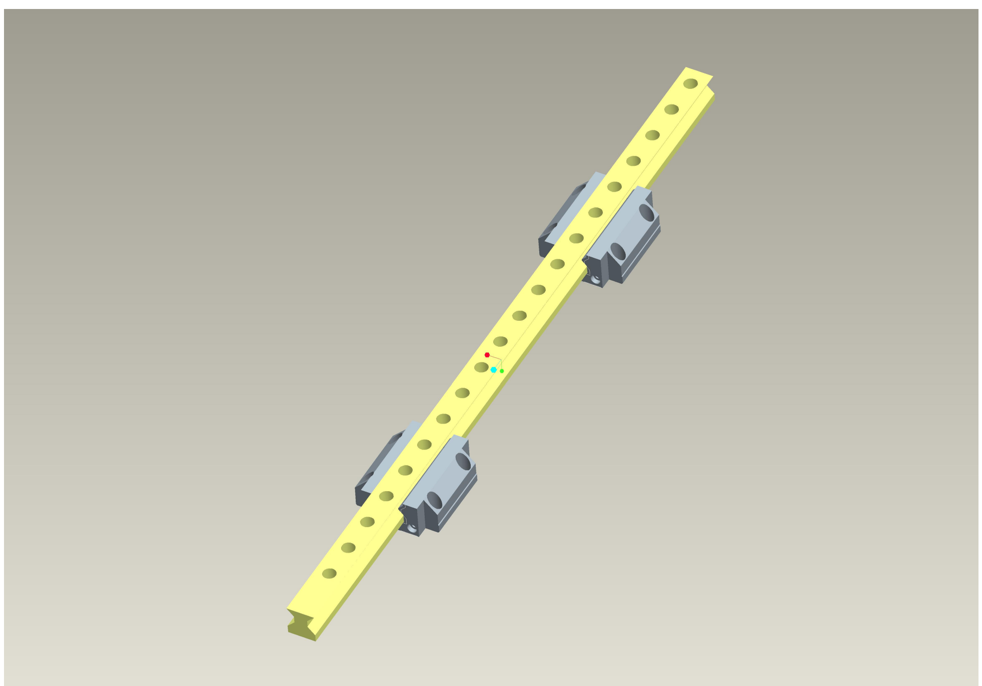

Figure 2.27 SCHNEEBERGER MRA 25 linear guide way assembly

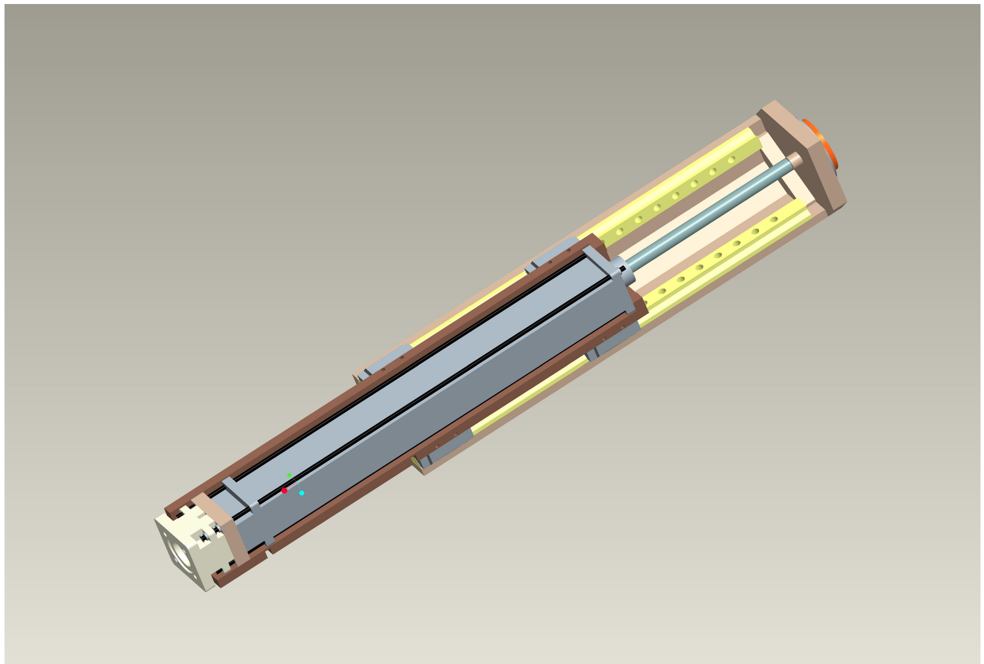

Figure 2.28 Linear Actuator with guides at the most critical operating condition

2.2.7 The Universal Joint and Bearing Assembly in order to have 3 degrees of freedom

In order to have three degrees of freedom on the top of the Stewart Platform, while obtaining the linear actuator and the top plate connection a gimbal system is required other than the two degrees of freedom universal joint assembly. Thus a bearing arrangement is embedded underneath the universal joint assembly. The universal joint assembly has maintained its freedom while having an extra degree of freedom with the bearing rotation.

In electromechanical systems using of bearings is critical. Since it would affect the system performance and might cause vulnerability in case of stiffness and controllability.

High precision, preloaded, duplex, angular contact, thin section ball bearings are used in back to back arrangement. The stiffness of the bearings which means the stiffness of the rolling elements inside the bearing is an important part of the overall characteristics of the dynamic operation of the system. Thus the bearings should be very stiff in order to avoid poor modal behavior and poor controllability of the system. Preloaded bearings are used in order to reach high stiffness. Back to back arrangement is done by pressing the outer rings with a retainer while having a small gap between the inner rings. This is the axial clearance coming from manufacturing tolerances. When the inner rings are pressed the gap is diminished and the bearings are preloaded to provide rigidity and high running accuracy. But there exists a tradeoff here. Since as the preload increases the stiffness of the system increases but also the friction increases. Optimum preload is selected using the manufacturer's catalogues. Lubrication plays an important role in bearing fiction. Low viscosity oil should be selected in order to have low friction. The bearings used in the system are lubricated in the manufacturing period and need to be lubricated periodically during their operating life. Ball separators used in the system also contribute to the overall bearing performance. Since the bearings are preloaded the friction effect of the separators is negligible. In order to apply low friction oil into the bearings a porous ball retainer should be selected. Figure 2.29 shows the spherical joint assembly.

The dimensional properties and load ratings of the bearings are as follows;

Outside Diameter: 88.9 mm
Width (pair): 12.7 mm
Static Radial Load Rating: 9416.2 N
Static Axial Load Rating: 8530.6 N
Weight: 118 g

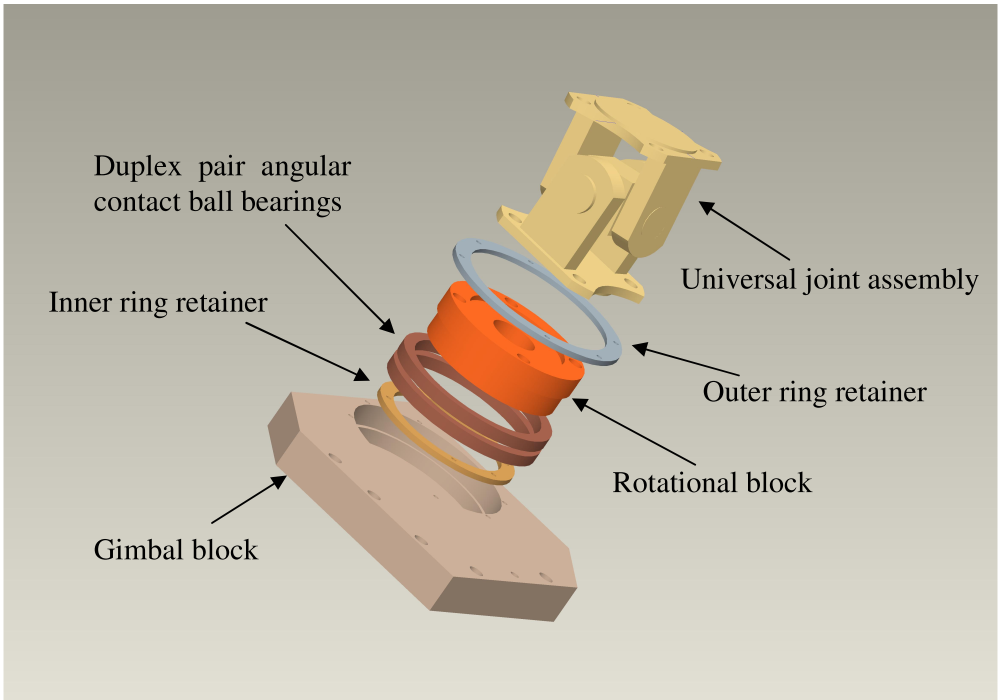

Figure 2.29 Spherical Joint assembly

As it can be seen from the figure an extra degree of freedom is added in the rotational sense which has a direction parallel to the vertical axis of the universal joint. The gimbal block is fixed to the linear actuator and the universal joint is fixed to the top plate by the connection holes via screws. Figure 2.30 shows the gimbal.

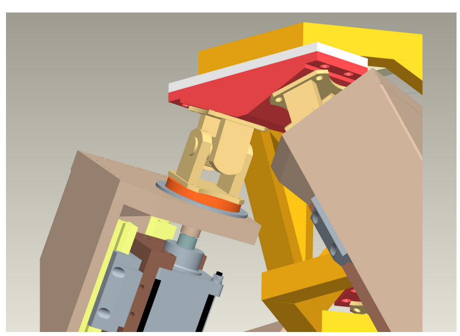

Figure 2.30 Gimbal under top frame assembly

2.2.8 Top Frame Assembly

Finally the top frame assembly is designed and constructed. The top frame assembly consists of top wedges, top plate and the adapter plates. The adapter plates are modular and interchangeable in case of any testing equipment. If the stabilized head mirror is tested the related adapter plate is used otherwise if the stabilized FLIR is tested the corresponding adapter plate is used. The stiffness of the top plate is very important as well as it should be lightweight, that is 11kg, for transportation issues. Modal analysis is performed in Chapter 2.3, Analysis 3, when designing the top plate and its stiffness has been guaranteed. The top wedges are used for the connection of the spherical gimbal to the upper platform. They do not require complex face angles since the initial position and free working area is performed by the wedges in the lower base. The top frame assembly can be easily dismounted from the spherical gimbals and the assembly of the testing equipment can be done outside far from the platform. Lightweight aluminum profiles have been used and welding process is applied on the mating surfaces. Figure 2.31 shows the top fame assembly.

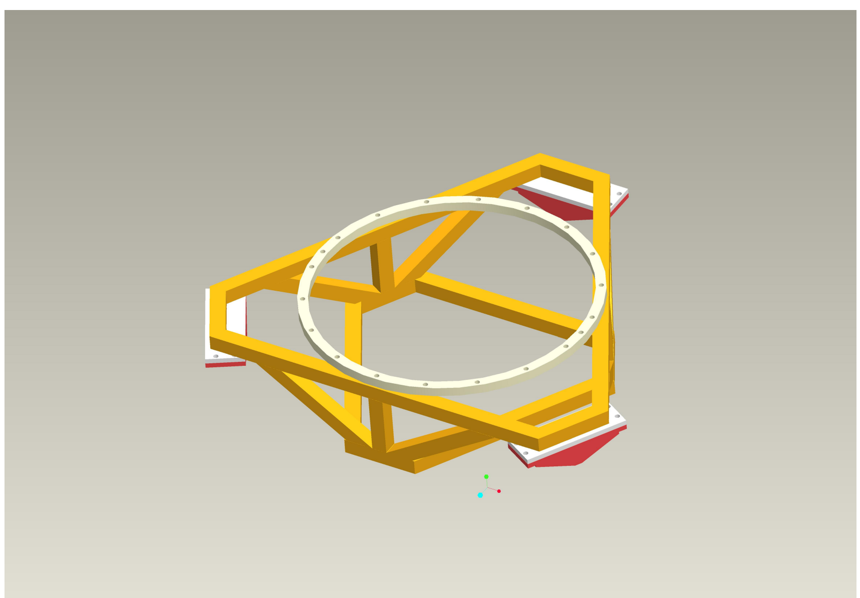

Figure 2.31 Top Frame assembly

With all the described parts and sub-assemblies the solid model is clear and ready for any modal analysis or virtual dynamic simulation by using related software. Although it consumes too much time and effort to prepare the solid model, it is worth to cope with since a perfect model is needed in analysis software. If the model breaks down easily multiples of time will be required to solve the problems faced in the analysis. Figure 2.32 shows the complete solid model of the Stewart Platform.

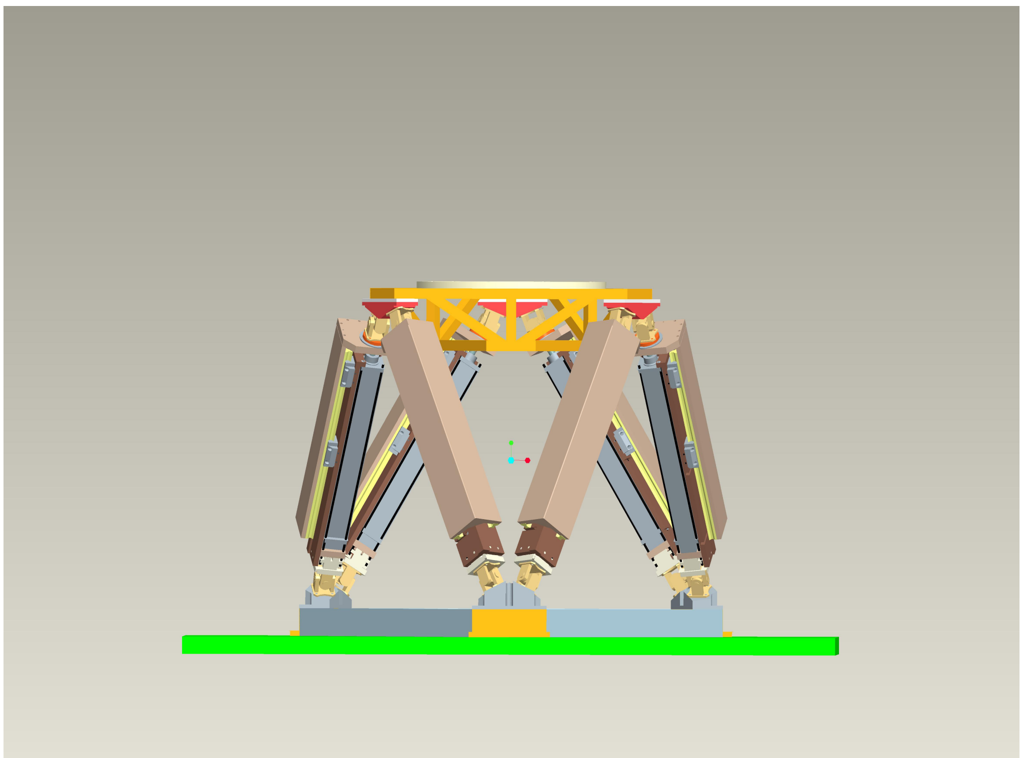

Figure 2.32 Solid model of the Stewart Platform

2.3 Modal Analysis of the critical parts

Since it is critical to have electromechanical equipment on land vehicles, the testing equipment should perform as close as possible to the real working environment. In order to perform as close as possible to the real working environment there has to be no noticeable phase lag or amplitude attenuation in the predefined operating range. This means that the bandwidth of the system should be clarified and the system should be operated in that frequency range. There are two important concepts in terms of mechanics that cause a system to fail or success to have high bandwidth. The first one is to have enough clearance between the mating parts. That is no other spacing should be other than the manufacturing tolerances between the mating parts. If the parts work in a sluggish manner the input that you embed into the system will not tend to create the desired output. This causes to have a lower bandwidth in contrast to system that is assembled perfectly according to the required manufacturing tolerances. The second one is the rigidity of the critical components which is directly related with the geometry of the parts and the material that the material has been manufactured from. In order to examine the second case finite element based modal simulation called frequency finder is used. The critical subassemblies that are prepared are imported into the finite element solver and all the material properties are defined, the contacts are implemented, required accelerations and loads are defined and the supports are charged into the required positions. After than a mesh is generated and the solution is observed. After little iteration, when the solutions tend to converge the results are obtained and the design is overviewed. In Analysis 1, the modal analysis of the linear actuator itself without the linear guides is presented. The linear guides are assembled next and the frequency spectrum is gathered once more. The expectation here is to have higher frequencies with the linear guides since the system becomes more rigid due to the housing effect of the linear guides other than the bushing effect of the housing of the shaft of the linear actuator. The other critical component in the assembly is the top frame. Since it has been produced from lightweight aluminum profiles for modularity it has to be examined in terms rigidity.

The assembly should be checked and if any discrepancy from the expectations is observed the geometry should be reconsidered.

Firstly the linear actuator's solid model is prepared without the linear guides. Some simplifications which will not affect the overall characteristics are made. The solid model is imported in the finite element solver. The analysis is named as Analysis 1 since it is important to define clear names to the analyses to check out if any modification is done to the solid model is regenerated in the finite element solver easily. Figure 2.33 shows the solid model of Analysis 1.

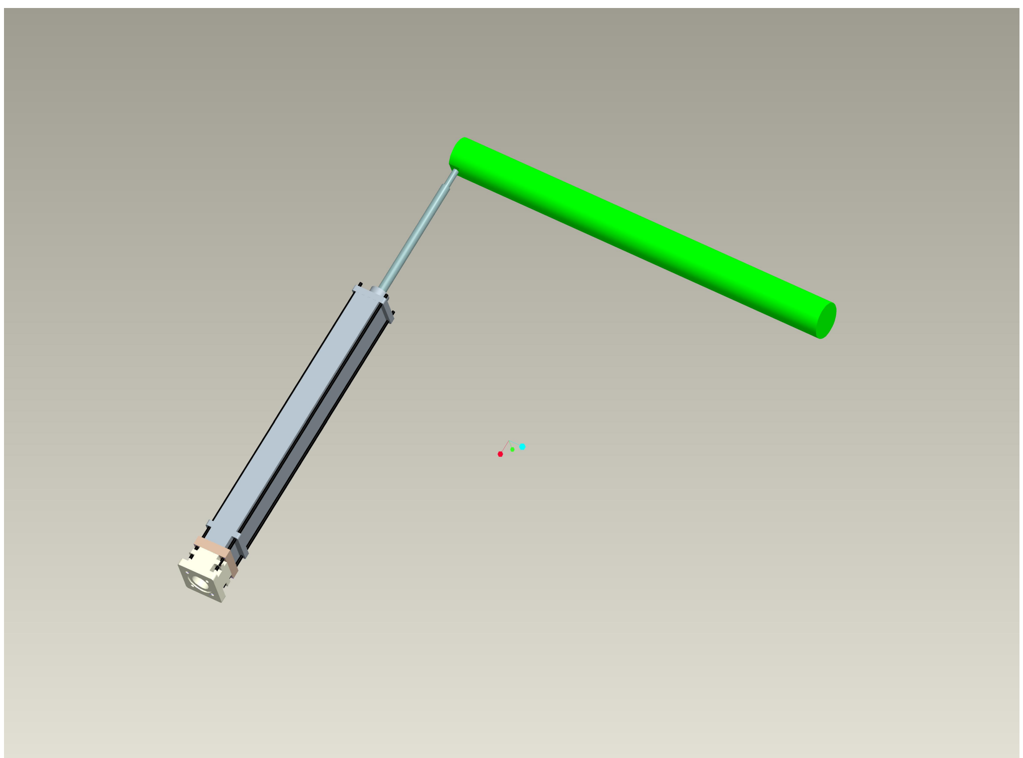

Figure 2.33 Solid model of Analysis 1

In order to create the actual loading conditions a dummy part has been created. This dummy part has its mechanical properties according to the designer. The actual payload of the system is divided into six to be shared by the six individual actuators. If the payload is considered;

Stabilized head mirror (the equipment that is going to be tested) = 20 kg,
Adapter plates = 20 kg,
Top plate = 20 kg,
Actuators = 60 kg all.

If the payload is shared equally 120/6 = 20 kg is weighted by each actuator. If a factor of safety of 1.5 is considered the load that each actuator will be faced becomes 30 kg.

The orientation of the payload is also critical. If the full assembly is considered the center of the payload is different from the actuators' line of operation. This can be shown like in Figure 2.34.

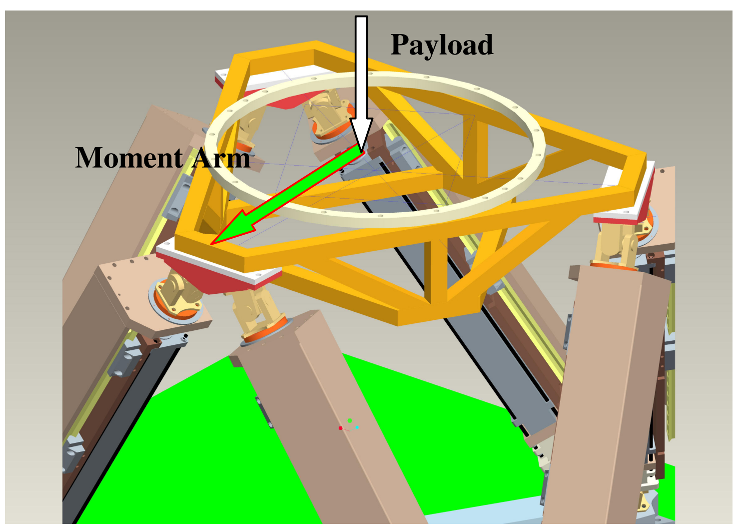

Figure 2.34 Loading on the Stewart Platform

Here payload that is shared by each actuator should be 30 kg where as the moment arm should be 455.2 mm as measured from the model. So the dummy part is considered as 30 kg mass and 910.4 mm tall symmetrical cylinder. Thus the loading will be like in Figure 2.35.

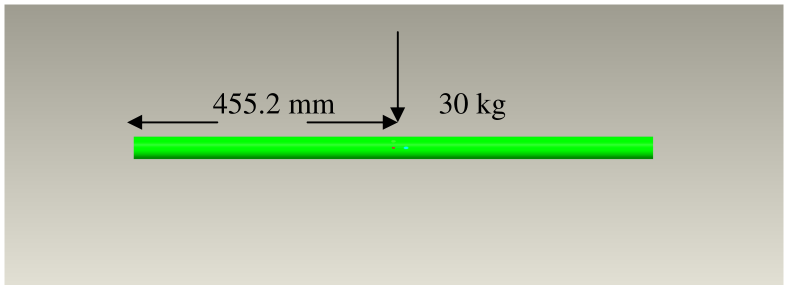

Figure 2.35 Dummy part

The mechanical properties of the dummy part should be selected carefully. It should be perfectly rigid so that the analysis will not interfere with the mode shapes or the characteristics of the dummy part. Dummy part will only stand for the actual loading conditions. For this reason the elastic modulus of the dummy part has been selected as 10^{13} Pa whereas stainless steel has an elastic modulus of 2×10^{11} Pa. The dummy part has an elastic modulus 500 times greater than the stainless steel. When the model is imported into the finite element solver the mechanical properties of each part should be neatly defined firstly. Figures 2.36 and 2.37 show the analysis environment.

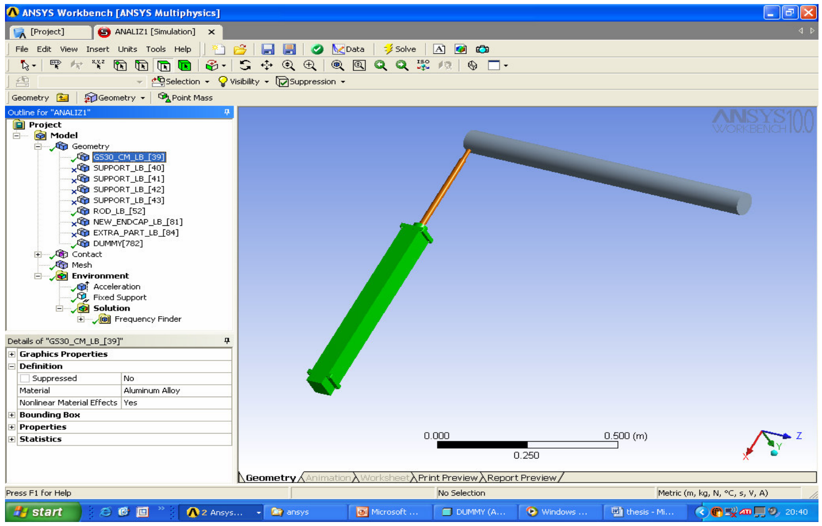

Figure 2.36 Defining material properties

After defining the material properties the necessary contacts will be defined. Contact tool can be applied to any assembly to verify the transfer of loads (forces or moments) across the various contact regions. Here the most important contact is between the actuator shaft and the actuator housing. The dummy part and the actuator shaft also have a contact at the tip of the dummy part.

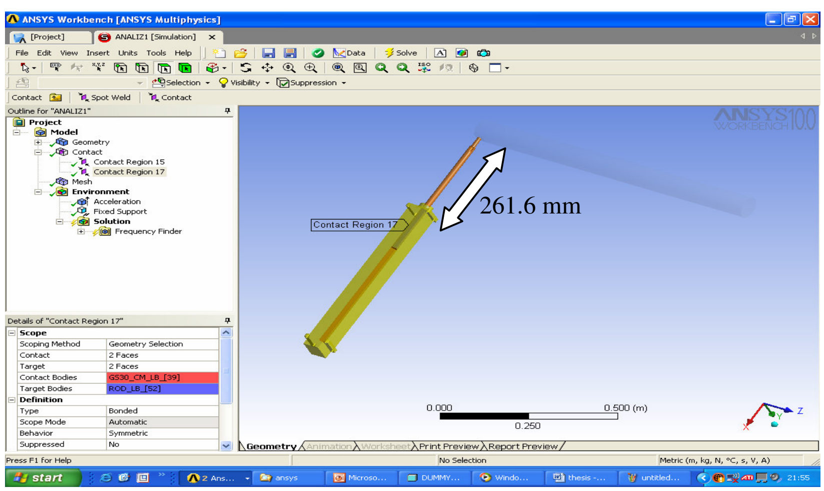

Figure 2.37 Defining contacts

If the figures 2.36 and 2.37 are examined carefully it can be seen that the analysis is done for the most critical case of the linear actuator. The most critical operating condition happens to appear when 261.6 mm distance occurs between the housing of the linear actuator and the tip of the shaft of the linear actuator. When the housing is fixed to the ground from its rectangular base and gravitational acceleration is defined in the direction of +X the model becomes ready to be solved and analyzed. If the solution is run the modal frequencies are found. The first four frequencies tell about the rigid body modes whereas the fifth frequency gives an impression about the modal characteristics of the system. The first natural frequency of the system is 83 Hz which seems not to be too low but the system should be improved to satisfy the expectations. The system should be as rigid as it can be up to the frequencies of 120 Hz which is the starting design criteria coming from the modal characteristics of the testing equipment and the field data collected when the tank is on the move. The sixth natural frequency is 109 Hz. When figures 2.38 and 2.39 that show the outputs of the ANSYS® software are examined, attention should be drawn to the dummy part. As it can be seen from the figures no modal displacement on the dummy part can be seen which ensures that the part is completely rigid in the range of analysis.

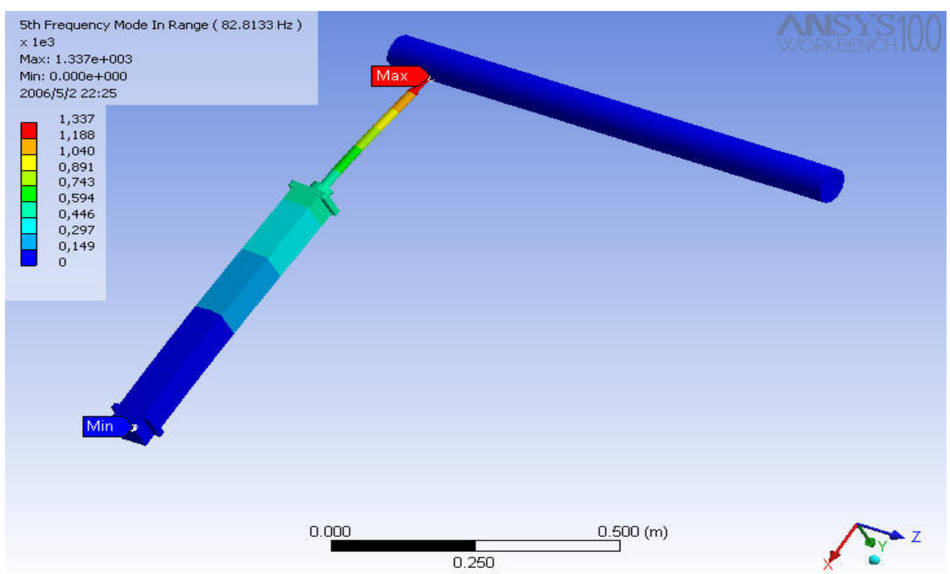

Figure 2.38 First flexible mode of Analysis 1

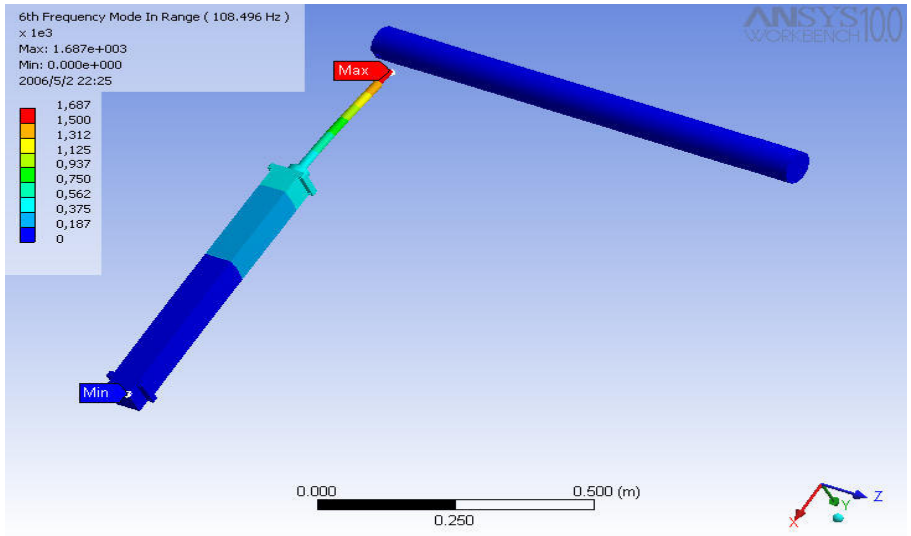

Figure 2.39 Second flexible mode of Analysis 1

As mentioned before the linear guideways should be implemented into the system in order to have single degree of freedom on the linear actuator (only translation). Other than supplying single degree of freedom to the linear actuator the linear guide ways will tend to increase the natural frequencies of the system. When the linear guide ways are implemented, the model is named as Analysis 2 in order to prevent confusions. Figure 2.40 shows the solid model of Analysis 2.

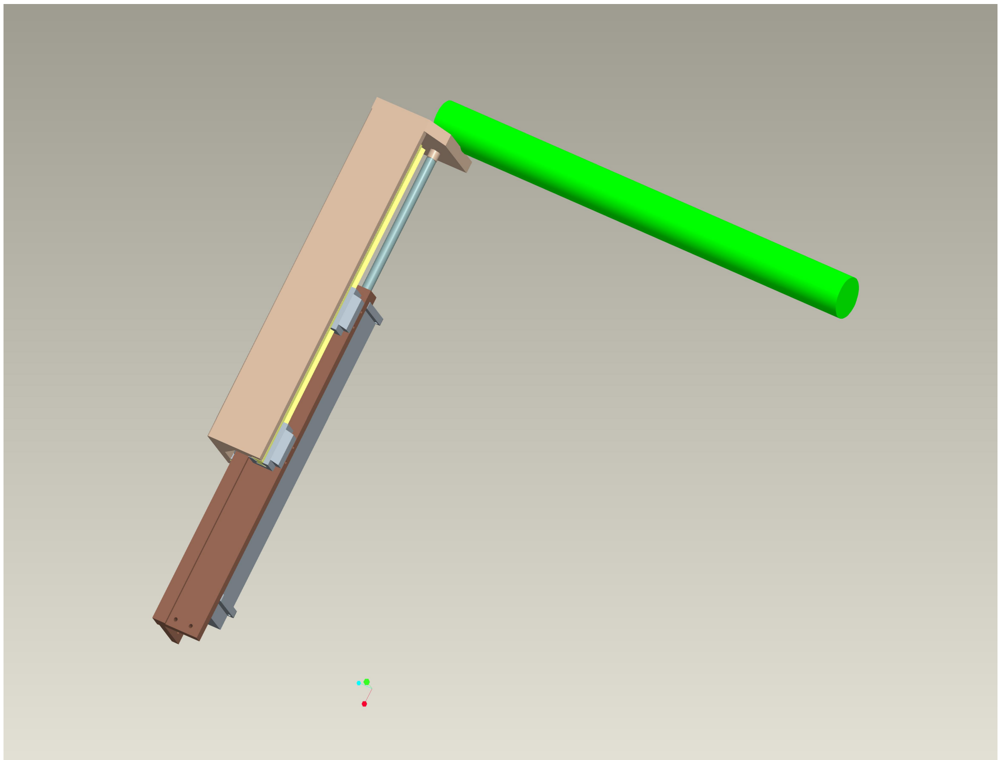

Figure 2.40 Solid model of Analysis 2

The fixed part of the linear guide way assembly that carries the carriages is shown in dark brown whereas the moving part of the linear guide way assembly that carries the rails is shown in light brown. The carriages and the rails are assembled and the material properties, contacts, gravitational acceleration and the fixement are defined in the finite element solver. The most important contacts embedded into the system with the linear guide ways are the contacts between the rails and the carriages. There are four contact regions between the rails and the guide ways in the most critical operating condition. Figure 2.41 shows the contact definition in Analysis 2.

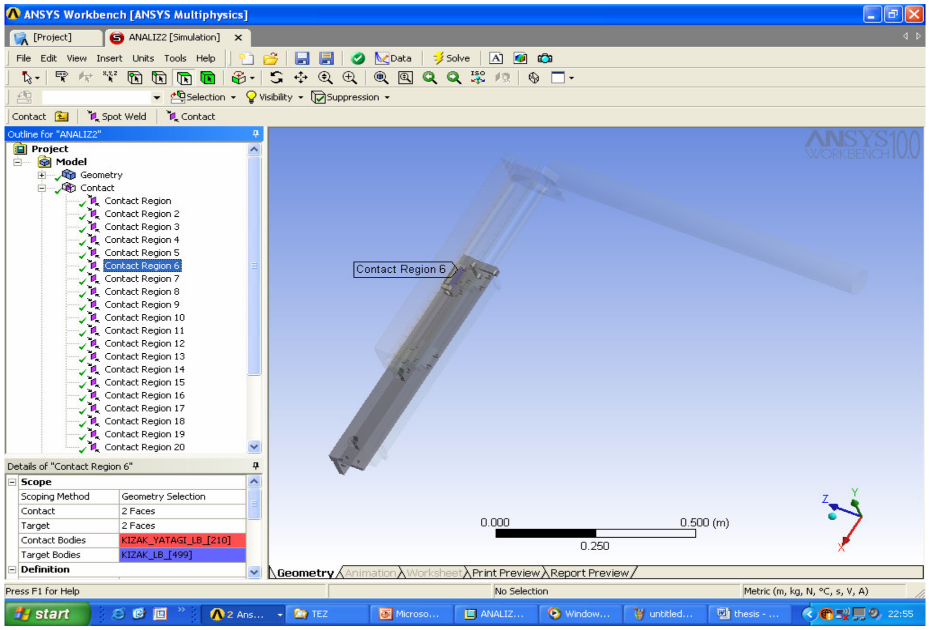

Figure 2.41 Defining contacts in Analysis 2

When the solution is run the expectation is to have higher natural frequency of the system from 83 Hz. The first four modes define the rigid body modes but fifth and sixth modes tell about the system characteristics. The first flexible mode of the system Analysis 2 is 201 Hz and the second flexible mode is 263 Hz. This means that the linear guideways have increased the natural frequencies up to the desired level while performing the single degree of freedom constraint of the linear actuator. Figures 2.42 and 2.43 show the exaggerated deflections of the parts at the natural frequencies. The other critical part is the top frame assembly and the finite element modal analysis is also done to this assembly. In any case of difference from the desired values of natural frequencies the design should be examined again and the necessary modifications should be done. The CAD software gives the opportunity of viewing the critical design parameters before manufacturing process. This eliminates the cost and relaxes the designer in terms of implementation of modifications. The flexible modes of Analysis 2 are as follows, shown in Figures 2.42 and 2.43.

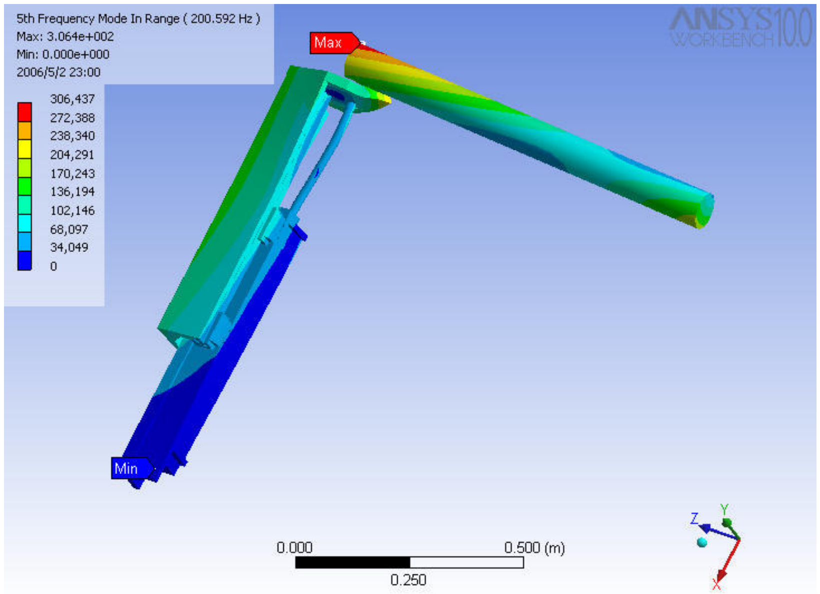

Figure 2.42 First flexible mode of Analysis 2

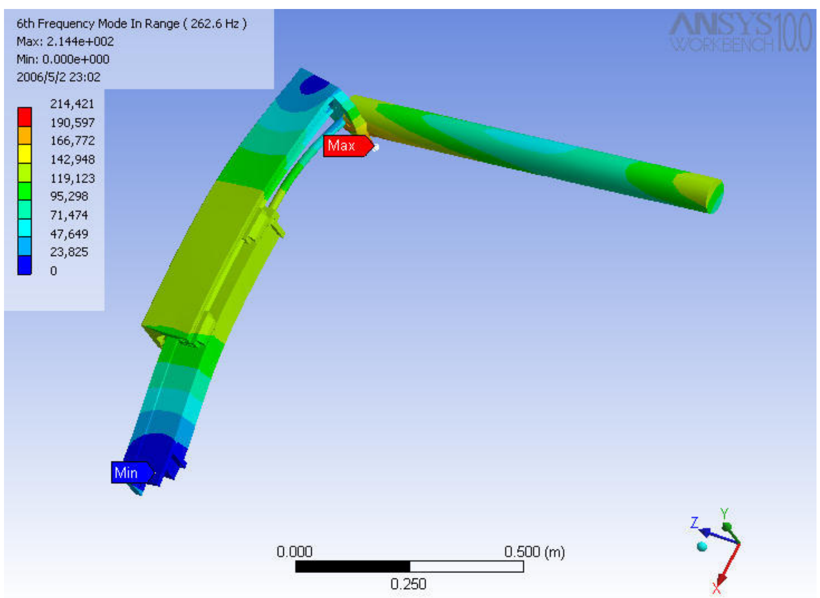

Figure 2.43 Second flexible mode of Analysis 2

The analysis of the top frame assembly is called as Analysis 3. The solid model is prepared and it is imported to the finite element solver. The solid model and the results are shown in Figures 2.44, 2.45, 2.46 and 2.47 below;

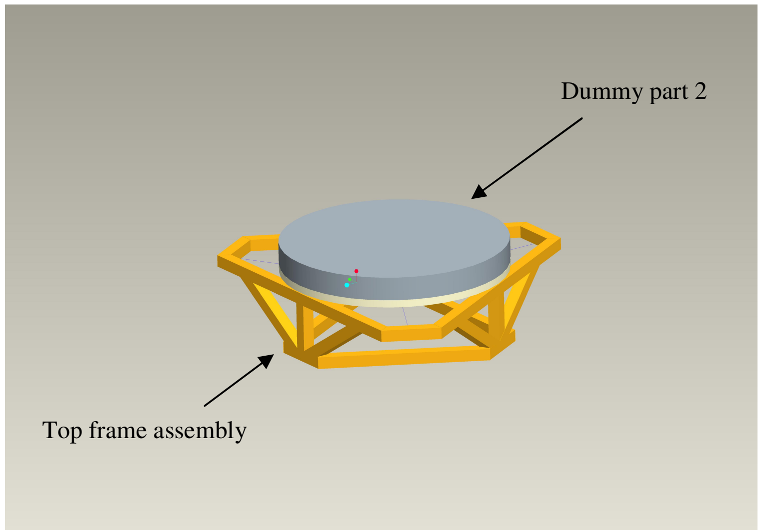

Figure 2.44 Solid model of Analysis 3

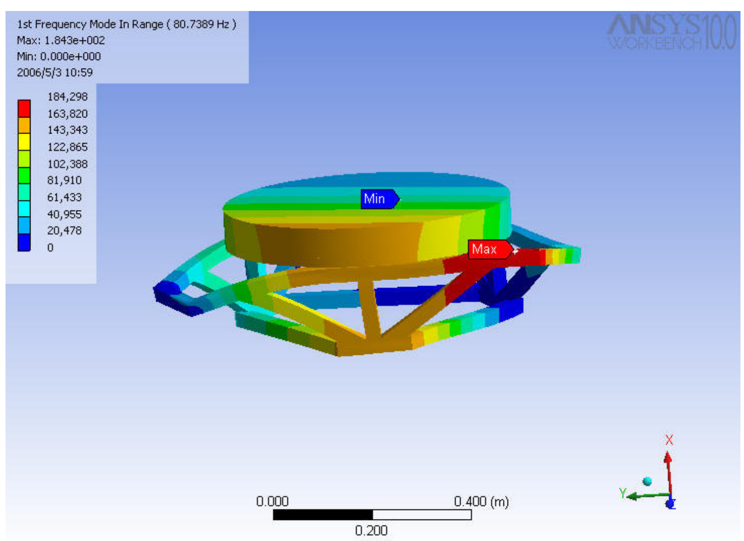

Figure 2.45 First flexible mode of Analysis 3

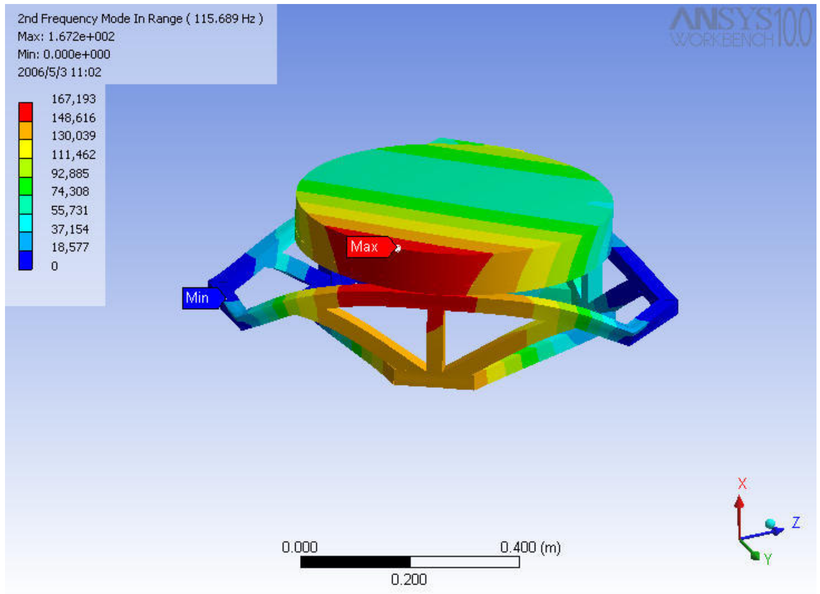

Figure 2.46 Second flexible mode of Analysis 3

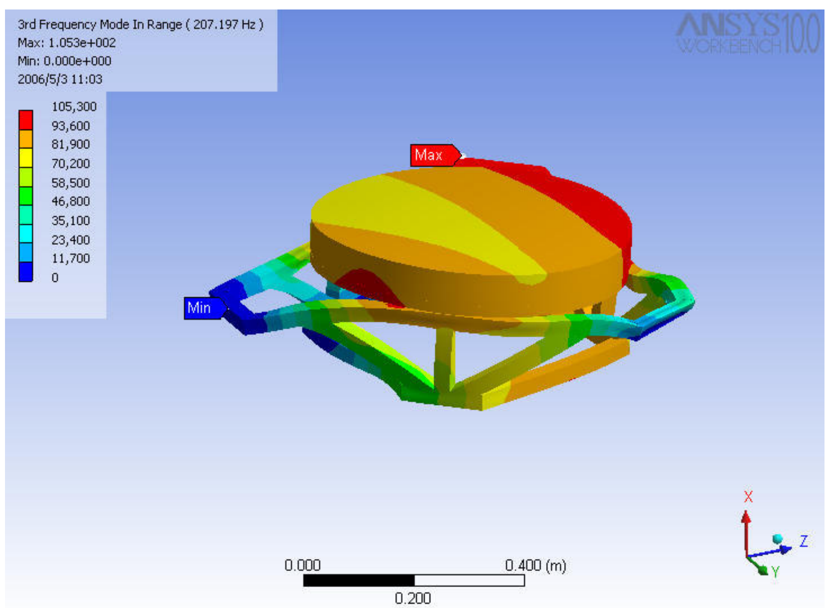

Figure 2.47 Third flexible mode of Analysis 3

The first three flexible modes are 81 Hz, 116 Hz and 208 Hz respectively. The first mode does not suffice to handle with the design criteria. When the analysis is examined carefully one important thing draws attraction. The assembly tends to deform through three edges where the fixed supports exist. The side supports do not perform well to hold the structure as rigid as desired. Then the design is modified and the side supports brought closer to the edges. Figure 2.48 shows the side view.

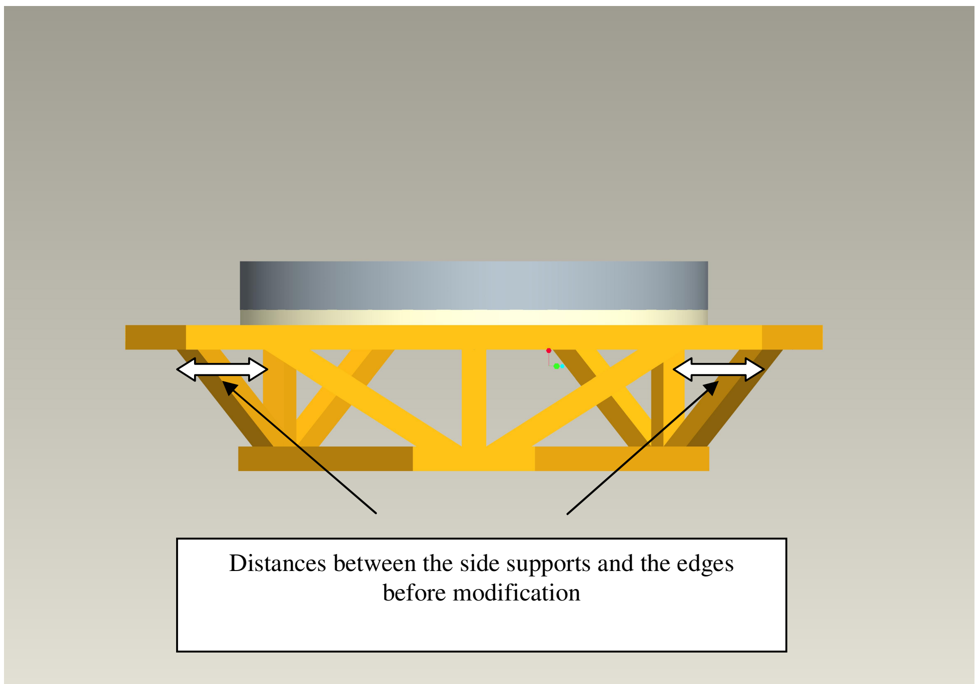

Figure 2.48 Side view of Analysis 3

After the distance between the side supports and the edges eliminated and the model is regenerated accordingly, the analysis is run again with the name Analysis 3_1. The results are not surprised and the flexible modes tend to go further to the safe side. The first flexible mode appears to be at 120 Hz whereas the second and the third one are 160 Hz and 167 Hz respectively.

The mode shapes are given in the Figures 2.49, 2.50 and 2.51;

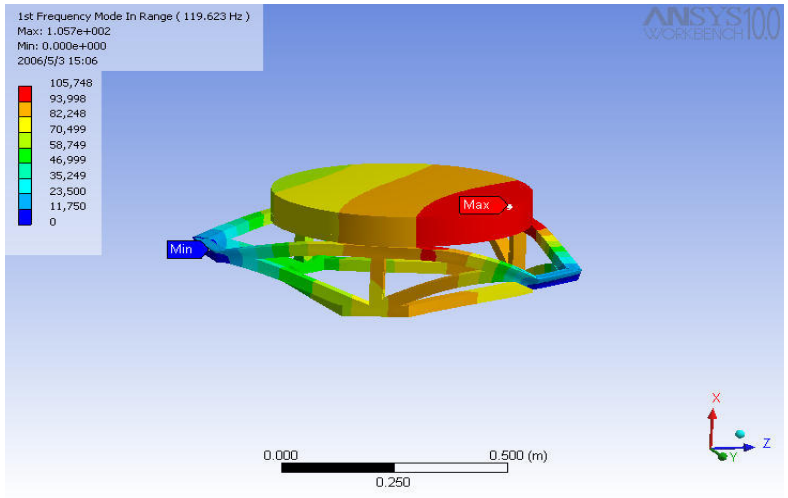

Figure 2.49 First flexible mode of Analysis 3_1

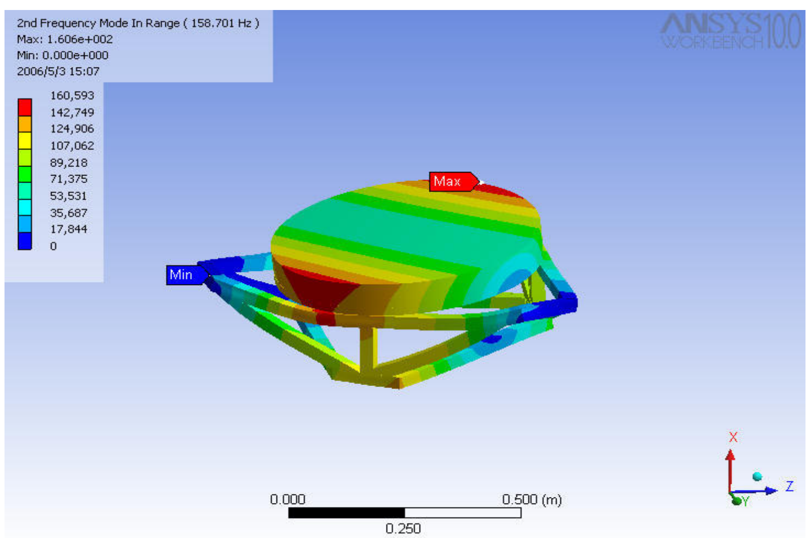

Figure 2.50 Second flexible mode of Analysis 3_1

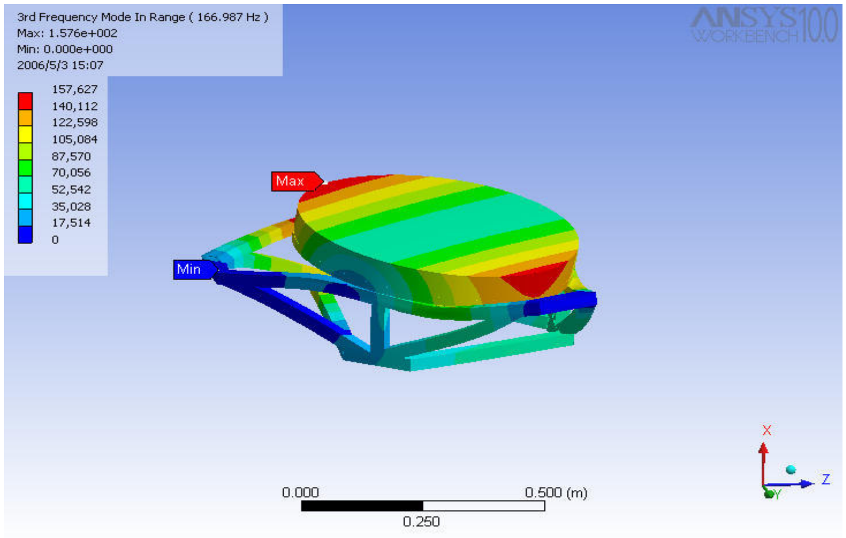

Figure 2.51 Third flexible mode of Analysis 3_1

The table that clearly shows the comparison between Analysis 1 and Analysis 2 can be seen underneath;

Table 2.1 Comparison table between Analysis 1 and Analysis 2

	Analysis 1 The linear actuator is analyzed with only its housing and shaft without the linear guideways	**Analysis 2** The linear actuator is analyzed with its housing, shaft and the embedded linear guideways
1st natural frequency (Hz)	83	201
2nd natural frequency (Hz)	109	263

The table that neatly describes the comparison between Analysis 3 and Analysis 3_1 can be seen underneath;

Table 2.2 Comparison table between Analysis 3 and Analysis 3_1

	Analysis 3 The top frame is analyzed with the side aluminum profiles are far from the edges	**Analysis 3_1** The top frame is analyzed with the side aluminum profiles are brought closer to the edges
1st natural frequency (Hz)	81	120
2nd natural frequency (Hz)	116	160
3rd natural frequency (Hz)	207	167

2.4 Virtual Mechanical Simulation of Stewart Platform

ADAMS/View® lets engineers build models of mechanical systems and simulate the full motion behavior of the models. It also lets to quickly analyze multiple design variations until the optimal design is reached. By this way a virtual prototype of any mechanical system can be built just as building the real physical prototype. The parts either can easily be created in the ADAMS® platform or imported from the CAD system, connecting with joints, assembling the system, and driving it with physically accurate forces and motions. The fidelity of the system may be improved by applying springs, dampers, contacts, and friction.

Parametric modeling is supported to evaluate multiple design ideas so that the model can be easily modified and used in design experiments. During the simulations, or when they are complete, ADAMS/View® provides the ability to animate the model's movement and view key physical measures of specific simulation data. This data emulates the data that would normally be produced physically.

Firstly the prepared solid model is imported carefully in the analysis environment. There are various ways to perform this operation. If the assembly is not too complex the solid model could easily be saved either .igs or .stp file in the modeling environment and imported into the analysis environment. But in a complex assembly case this would not work. The assembly should be saved in format that none of the components should leave their properties out. This is the .xmt format. The assembly is saved as .xmt and imported into the analysis environment. If the assembly was not saved and imported as .xmt the components would not be clarified in the database navigator of the program. The imported assembly is shown in Figure 2.52.

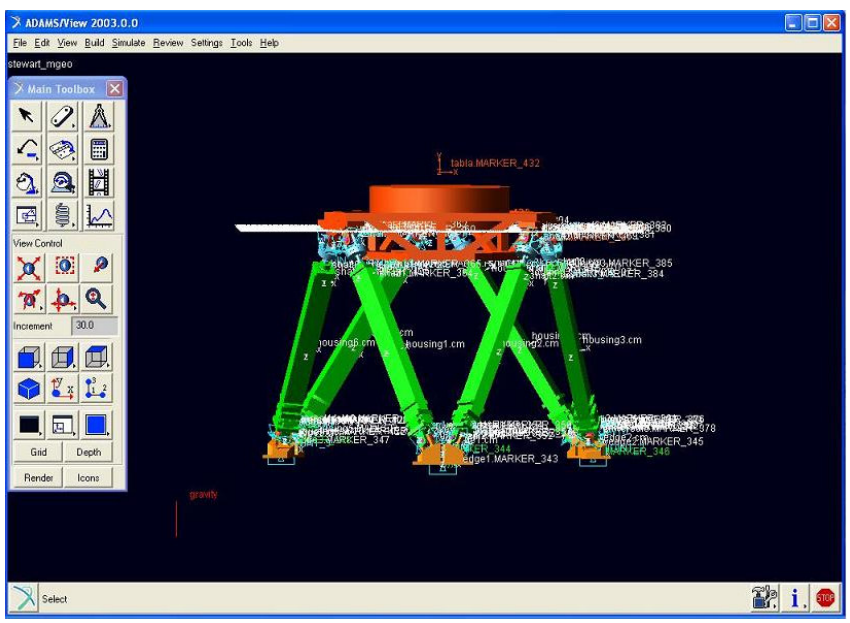

Figure 2.52 Stewart Platform in ADAMS® 2003

In order to perform mechanical analysis and simulation firstly the joints between the components should be defined neatly. The base should be fixed to the ground with fixed support. Figure 2.53 shows the fixed joint.

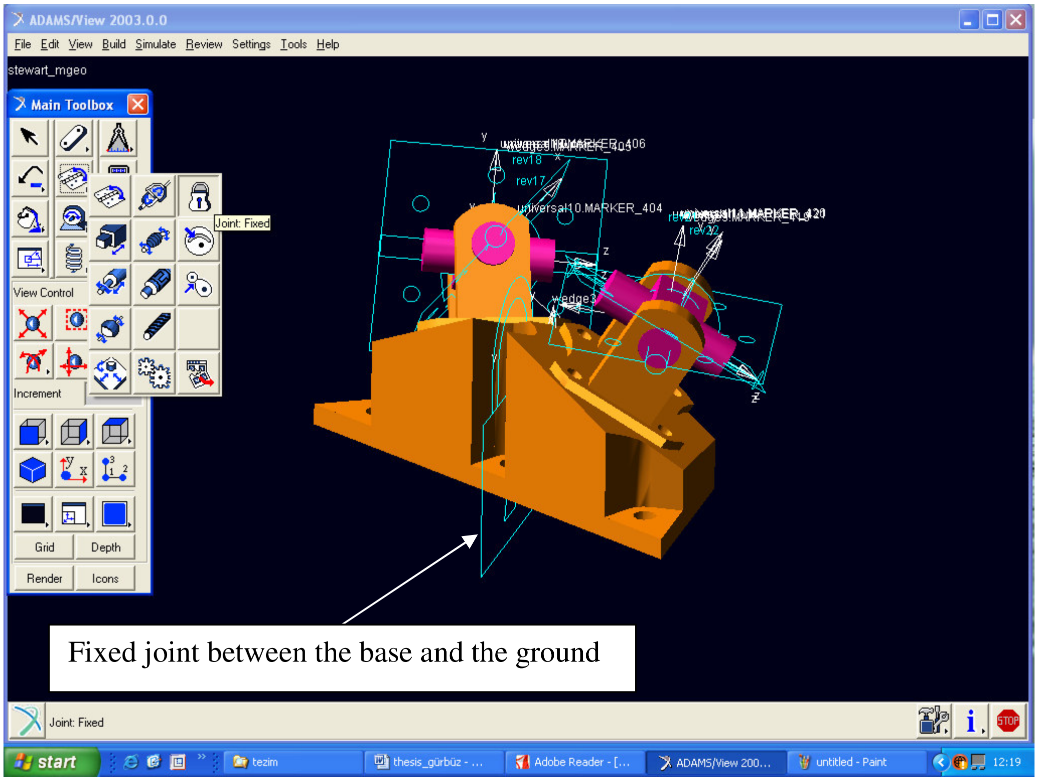

Figure 2.58 Fixed joint between the base and the ground

Fixed joint implies full non motion constraint on all of six degrees of freedom on the base and the base is merged with the ground. Nor translational neither angular acceleration would move or rotate the base. The aluminum profiled columns are not imported in order to simplify the assembly. The three wedges are standing at the bottom of the assembly as in the real physical case. The universal joints are fixed on the wedges whereas the mechanics of the universal joints are defined as follows in Figure 2.54.

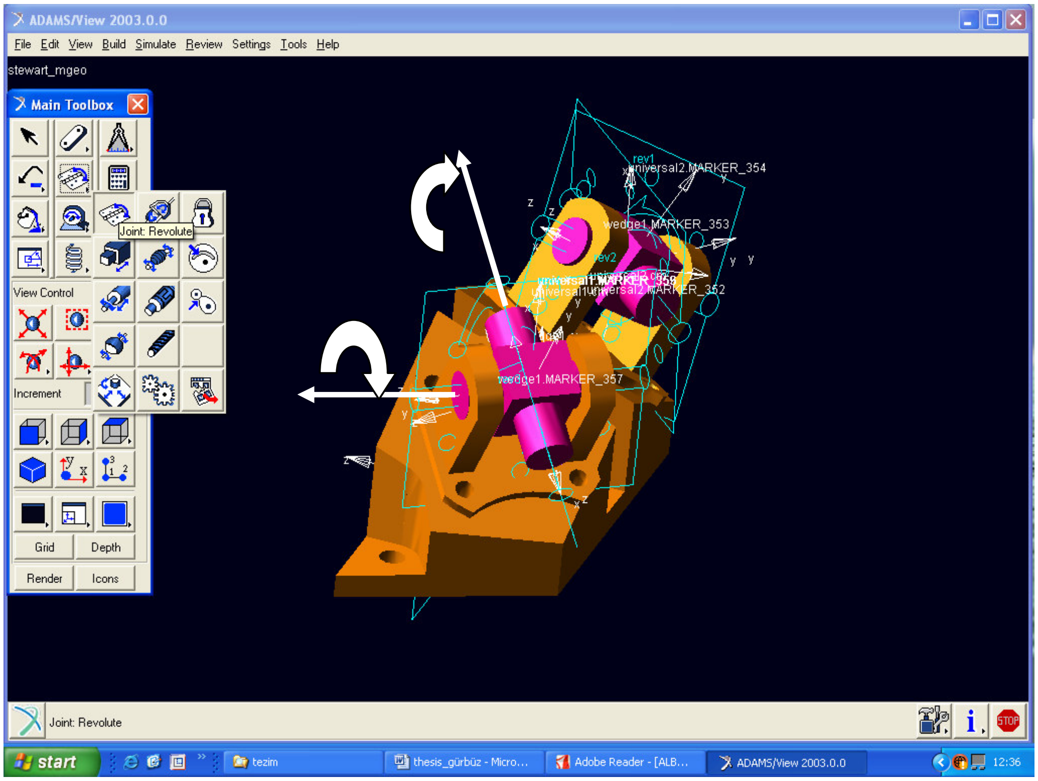

Figure 2.54 Two rotational degrees of freedom on the universal joints

The revolute joint fixes three of the translation and two of the rotational degrees of freedom whereas it relaxes one of the rotational degree of freedom in the desired direction as shown in Figure 2.46. In the universal joint there exist two rotational degrees of freedom. Two revolute joints are superimposed individually and the universal joint is formed. One of the other joints is the prismatic joint between the housing of the linear actuator and the shaft of the linear actuator. In order to simplify the model and the analysis a cylindrical joint is defined between the housing and the shaft which would not diverge the model from the real mechanical system, whereas it would simplify the model and make the solution time shorter. It would enable both translation and rotational degrees of freedom between the housing and the shaft. An insight into the joint can be seen in Figure 2.55.

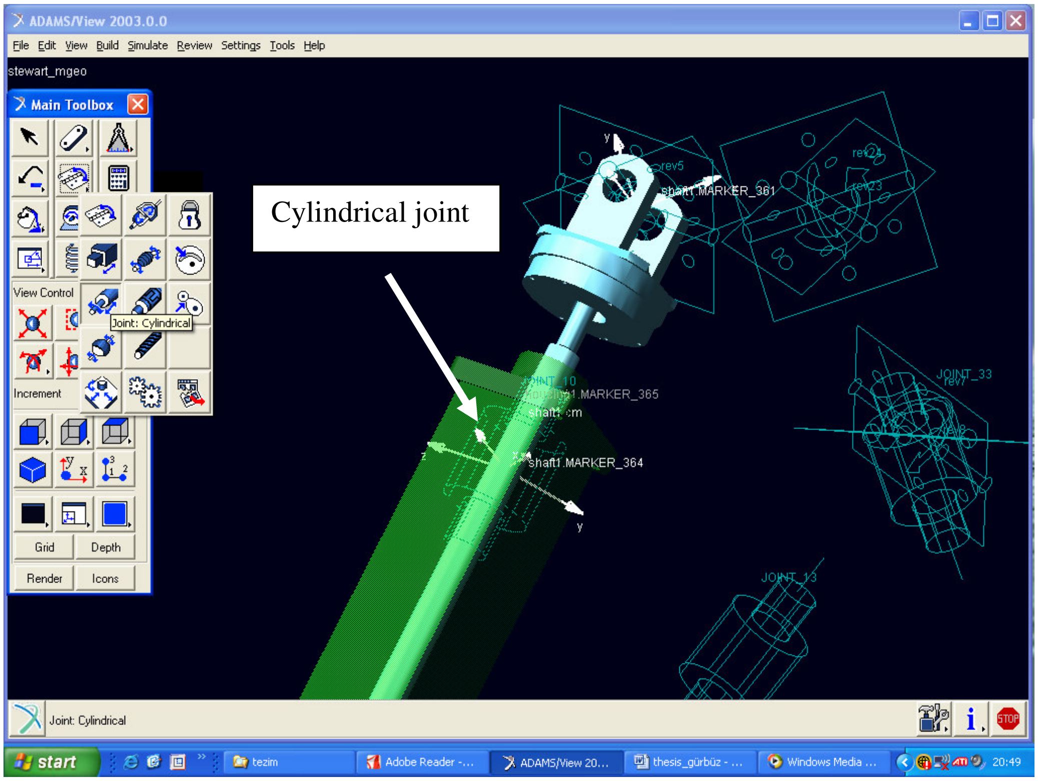

Figure 2.55 Cylindrical joint between housing of the linear actuator and the shaft of the linear actuator

The upper universal joints are defined as the same as the bottom universal joints. All of the joints should be defined one by one in order to prevent confusions and the model should be verified mechanically each time. The platform makes its own degree of freedom calculation and gives a warning if there exists a contradiction.

As it was done in the modal analysis case a proper loading should be defined with a dummy mass. The dummy mass would be fixed to the upper platform and it would have the mass properties same as the payload. It would act at the center of gravity of the system. A cylindrical dummy weight is preferred in order to distribute the payload homogenously. Figure 2.56 shows the dummy weight and the upper platform.

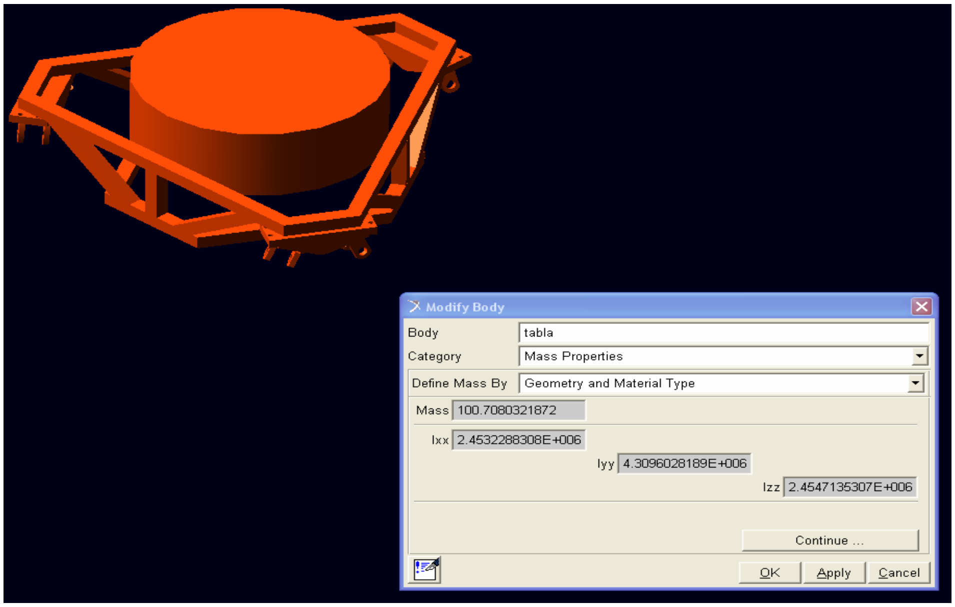

Figure 2.56 Dummy weight and the upper platform

The joints between the components and the proper loading are defined. Now there has to be a proper motion in order to measure the characteristics in working space and payload considerations in the design criteria. The motion is found from the collected road data of the tank both in elevation and azimuth axes. The tank is driven in the field and the required motion data is gathered from the gyroscopes. Firstly the elevation axis is considered and the colleted data is superpositioned in order to create a general motion that would be given to the prepared model. The motion could easily be defined in the ADAMS® environment and a simulation is run.

The simulation results are plotted and observed both in translational displacement and linear thrust values. In the elevation axis with the superpositioned data the critical linear displacement that the actuators are faced with is 260 mm whereas the critical linear thrust is 500 N. If the catalogue values are observed maximum linear displacement of the linear actuators is 450 mm. The linear thrust is 3000 N.

The superpositioned elevation general motion data is as follows in Figure 2.57.

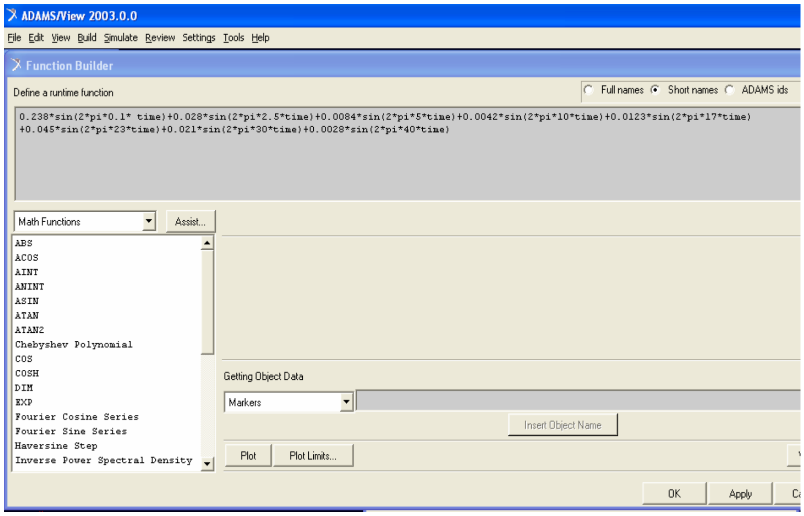

Figure 2.57 General motion definition in elevation axis

The general motion can be viewed in Figure 2.58.

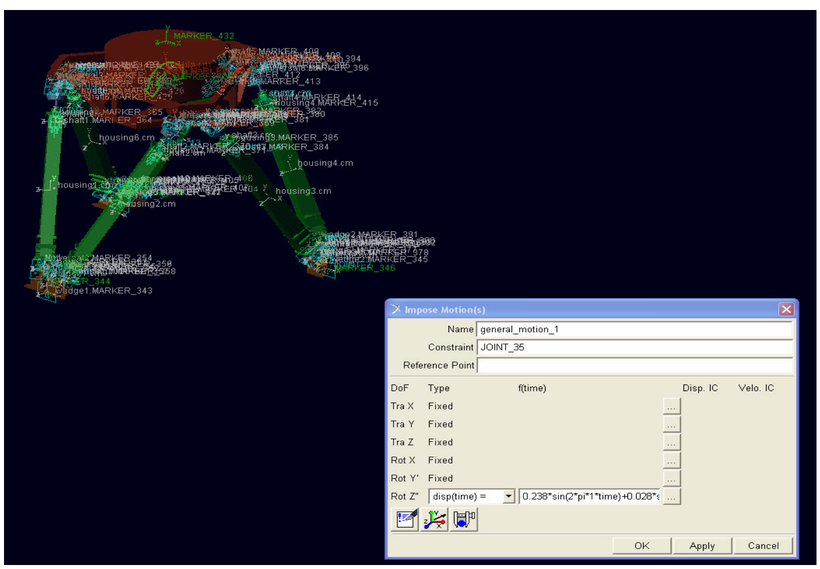

Figure 2.58 General motion in elevation axis

The graphical observation of the linear displacement results of the linear actuators in the simulation of the model in elevation axis is as follows in Figure 2.59.

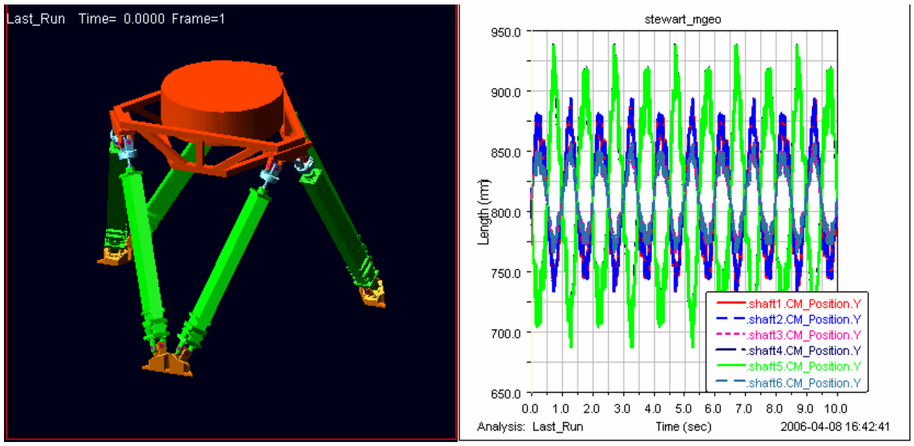

Figure 2.59 Linear displacement values of the linear actuators in the elevation general motion data

The graphical observation of the linear thrust results of the linear actuators in the simulation of the model in elevation axis is as follows in Figure 2.60.

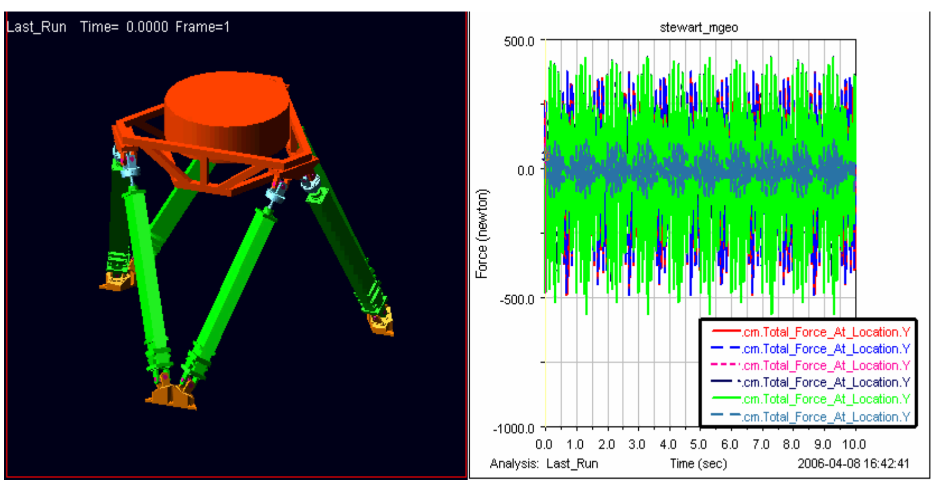

Figure 2.60 Linear thrust values of the linear actuators in the elevation general motion data

If the same logic is applied in the azimuth axis, that is to say if the collected azimuth motion data is superpositioned and applied on the prepared model as a general motion, the critical linear displacement value of the linear actuators is 50 mm whereas the critical linear thrust value of the linear actuators is 25 N shown in Figures 2.61 and 2.62.

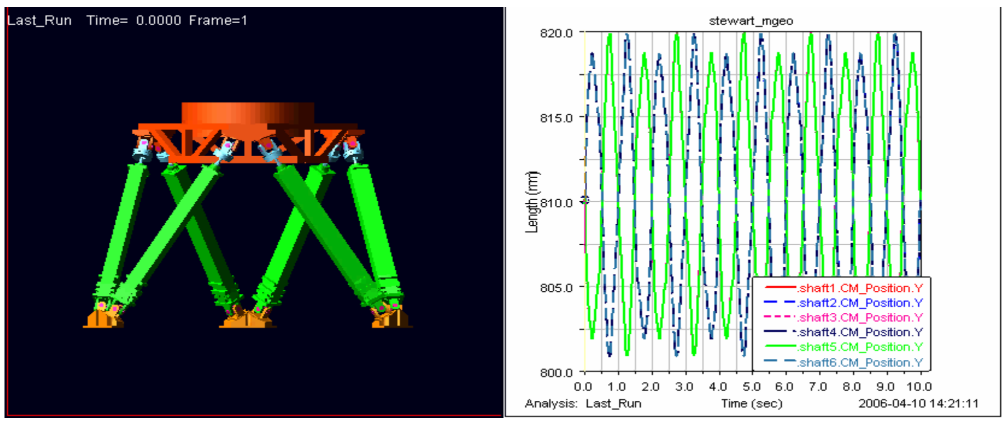

Figure 2.61 Linear displacement values of the linear actuators in the azimuth general motion data

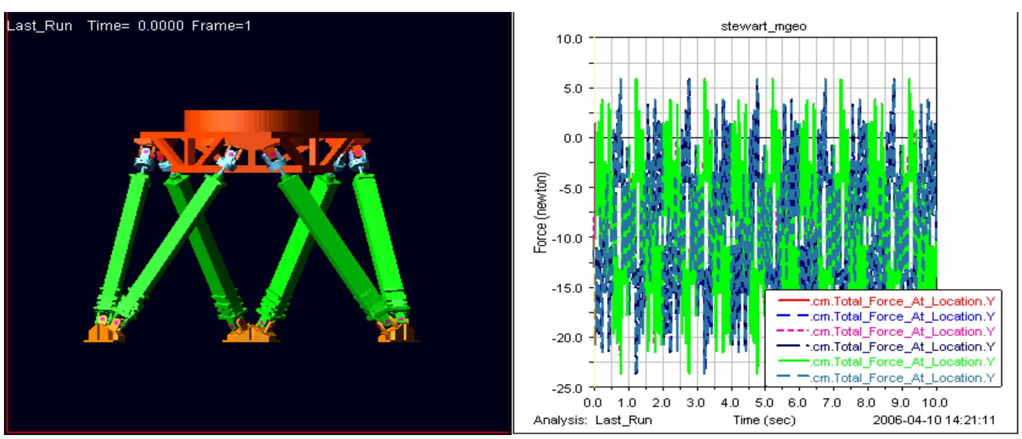

Figure 2.62 Linear thrust values of the linear actuators in the azimuth general motion

If a comparison is done again with the catalogue values it can be verified that the azimuth values are not as critical as the elevation values. So that the actuators are safe to use both in working space and payload design criteria.

All of the work described above is unique and an important example for the virtual product development. The most important aspect of the virtual product development is saving time and money. The final physical prototype is not manufactured until successful design parameters are reached in the virtual prototype. When desired values are reached, the final physical prototype can be manufactured and tested in the real environment since there happens to be some deviations from the virtual product. These deviations should be overwhelmed in the testing period.

The design period is very complex and confusing without the use of CAD tools. However these tools should be used very carefully and designer should always be suspicious with the values gathered from the design tools. The real physical prototype should be tested and observed neatly in order to measure the real design values. A successful design is reached when the design values of the CAD tools and the real physical prototype does not differ ultimately. Six degree of freedom simulator is widely and effectively in ASELSAN environment as testing equipment and is a very good example for the virtual product development in ASELSAN facilities.

CHAPTER 3

MAXIMUM PAYLOAD INVESTIGATION

Stewart Platform is a mechanical dynamic system. As explained before this system is used for testing purposes. The main function of this testing system is to create a motion trajectory for the testing equipment. The equipment that is tested on the platform plays an important role in the mechanical characteristics of the platform. There has to be a specified payload value on the testing equipment. This value is specified as 120 kg in Chapter 2. But there has to be a payload value that should be given in order to describe the platform's working limit. At that payload value one of the platform's critical parts should deform plastically and the platform should become unusable. This payload value is named as the maximum payload that the platform should carry in the normal operating conditions. The investigation of the maximum payload is a tedious process with effective and maximum using of the CAD software. When the dynamic loading is applied on the platform with a dummy weight with the specified testing motion trajectory a stress analysis is carried on the critical parts in order to find if there exists a failure or not. The critical parts are the top frame and the six individual shafts of the linear actuators. The payload is increased gradually and after each increase the Von-Mises stress values on the critical parts are reported. The reported stress values are compared with the yield stress values of the materials of the critical parts and continued until the values go beyond the critical values. In order to investigate the maximum payload ADAMS/View®, ADAMS/Flex® and ADAMS/Autoflex® and ADAMS/Durability® software are used. ADAMS/View® is used to model the variable dummy weight. ADAMS/Flex® is used to assign the mesh properties of the top frame. Firstly ANSYS® is used to create the .mnf (modal neutral file) of the top frame which carries the modal properties of the top frame with specified mesh properties. Then this .mnf file is introduced into ADAMS® by using ADAMS/Flex®. ADAMS/Autoflex® is used to transform the rigid actuator shafts into flexible. Autoflex® can assign mesh properties and form a .mnf file without requiring any other finite element solver. This program directly creates a mesh and edits the attachments of the part in the assembly. ADAMS/Durability® is used to report the stress values and observe the results. The dummy weight is modeled as two concentric cylinders which represent the real payload as closely as possible. The initial payload value is set to be 150 kg which is slightly greater than the design criteria brings the important point. At this payload value the system will not behave well since it will not pass the modal design criteria with this much payload. However the investigation is done in order to find out the maximum payload that the system will carry without any failure. The maximum payload with the required modal behavior and rigidity is 120 kg as specified before. The meshing capability of ADAMS/Autoflex® is shown in Figure 3.1. Figure 3.2 shows the flowchart of the investigation process.

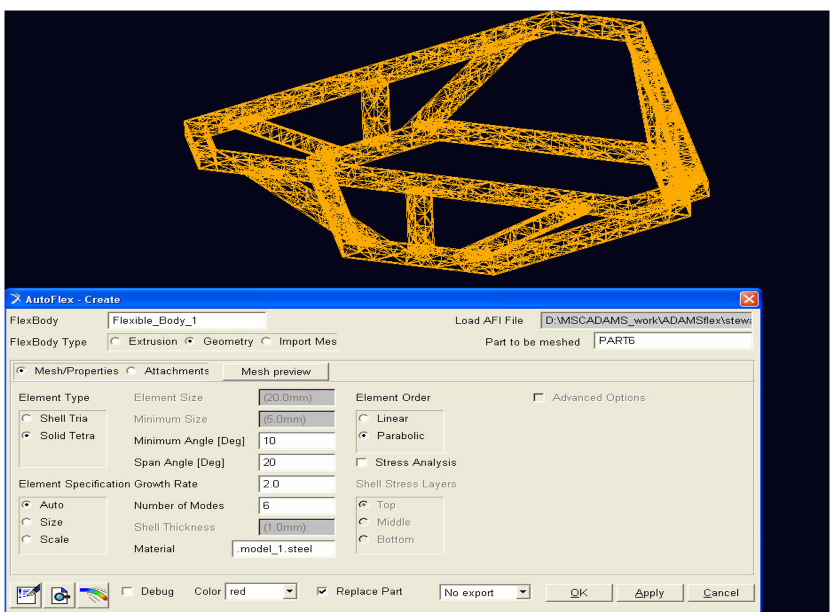

Figure 3.1 Top frame meshed in ADAMS/Autoflex®

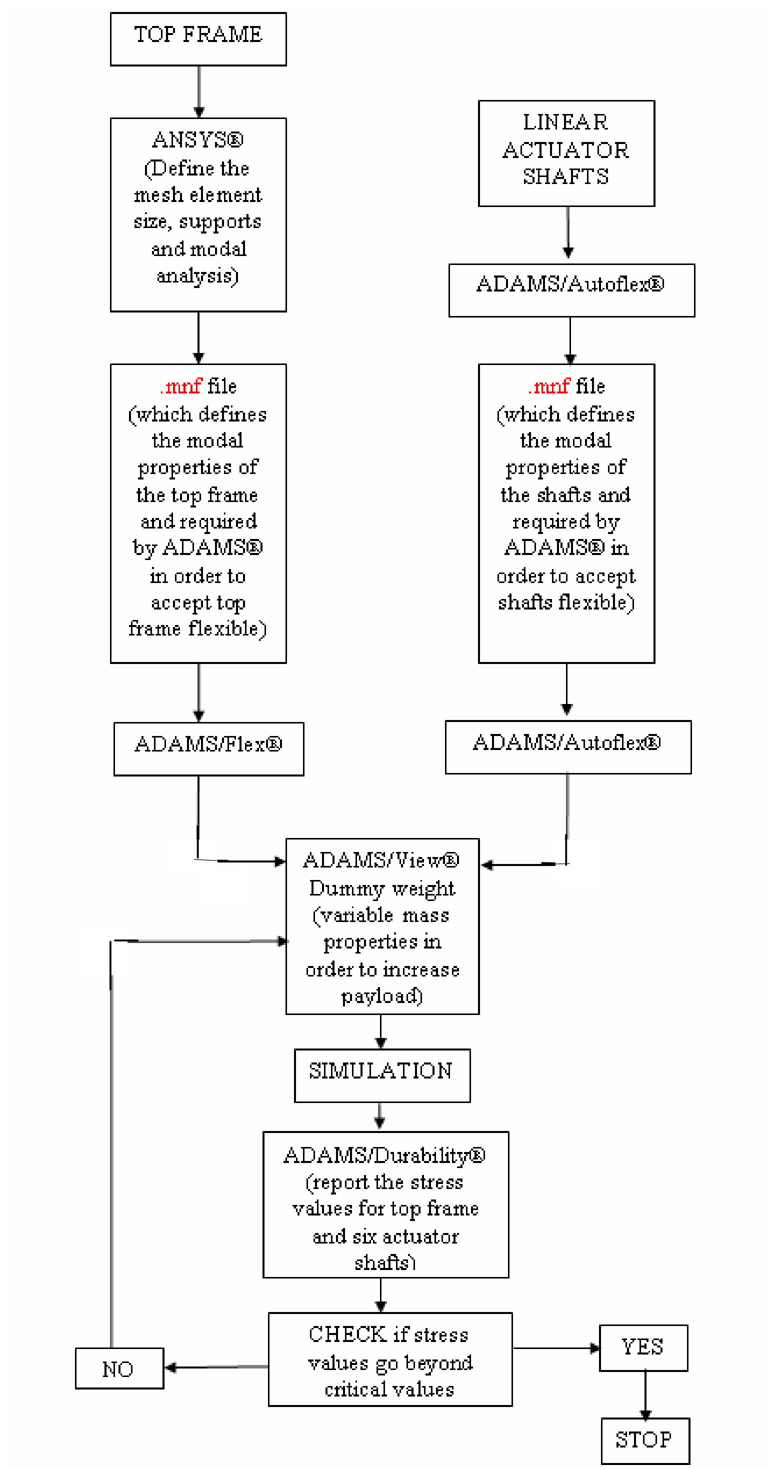

Figure 3.2 Flowchart of the maximum payload investigation

The dummy weight's solid model geometry and orientation is fixed since it reflects the center of gravity and the inertia tensor of the real physical system as closely as possible. Only the density of the payload is changed in order to increase the weight and observe the deviations in the Von-Mises stresses. When the simulation is run with the 150 kg payload the observed stress values on one of the flexible linear actuator shaft is described below. Figure 3.3 shows the analysis results with 150 kg.

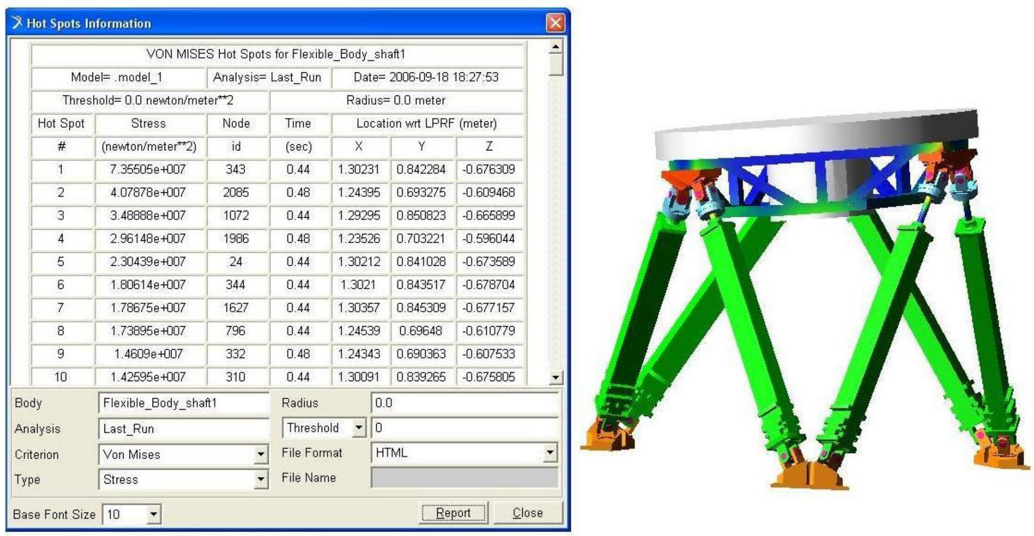

VON MISES Hot Spots for Flexible_Body_shaft1

Model= .model_1 | Analysis= Last_Run | Date= 2006-09-18 18:27:53

Threshold= 0.0 newton/meter**2 | Radius= 0.0 meter

Hot Spot #	Stress (newton/meter**2)	Node id	Time (sec)	Location wrt LPRF (meter) X	Y	Z
1	7.35505e+007	343	0.44	1.30231	0.842284	-0.676309
2	4.07878e+007	2085	0.48	1.24395	0.693275	-0.609468
3	3.48888e+007	1072	0.44	1.29295	0.850823	-0.665899
4	2.96148e+007	1986	0.48	1.23526	0.703221	-0.596044
5	2.30439e+007	24	0.44	1.30212	0.841028	-0.673589
6	1.80614e+007	344	0.44	1.3021	0.843517	-0.678704
7	1.78675e+007	1627	0.44	1.30357	0.845309	-0.677157
8	1.73895e+007	796	0.44	1.24539	0.69648	-0.610779
9	1.4609e+007	332	0.48	1.24343	0.690363	-0.607533
10	1.42595e+007	310	0.44	1.30091	0.839265	-0.675805

Figure 3.3 Von-Mises Stress values on the flexible shaft during testing simulation under 150 kg payload

As it can be seen from the hot spots table gathered from the ADAMS/Durability® software the maximum stress appeared on the flexible shaft is 73.5 MPa. The material of the actuator shaft is AISI 304 stainless steel which has a yielding stress of 215 MPa. The payload can be increased further since the shaft has not passed into plastic deformation region yet. On the other hand, the stress values on the top frame should be observed at the same time. The stress values on the top frame during the same simulation is shown in Figure 3.4.

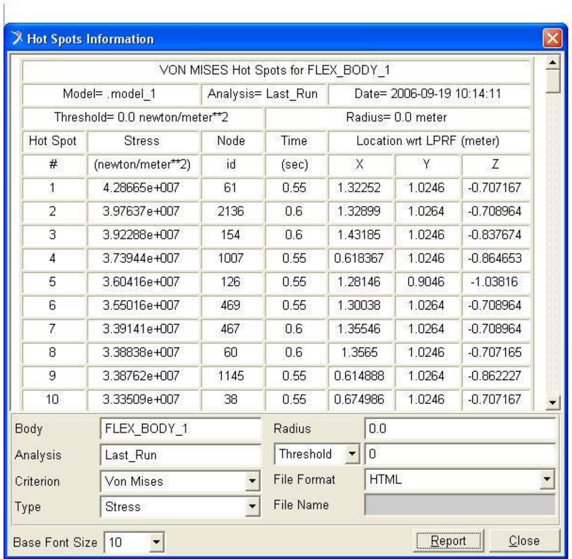

Hot Spots Information

VON MISES Hot Spots for FLEX_BODY_1						
Model= .model_1	Analysis= Last_Run		Date= 2006-09-19 10:14:11			
Threshold= 0.0 newton/meter**2			Radius= 0.0 meter			
Hot Spot	Stress	Node	Time	Location wrt LPRF (meter)		
#	(newton/meter**2)	id	(sec)	X	Y	Z
1	4.28665e+007	61	0.55	1.32252	1.0246	-0.707167
2	3.97637e+007	2136	0.6	1.32899	1.0264	-0.708964
3	3.92288e+007	154	0.6	1.43185	1.0246	-0.837674
4	3.73944e+007	1007	0.55	0.618367	1.0246	-0.864653
5	3.60416e+007	126	0.55	1.28146	0.9046	-1.03816
6	3.55016e+007	469	0.55	1.30038	1.0264	-0.708964
7	3.39141e+007	467	0.6	1.35546	1.0264	-0.708964
8	3.38838e+007	60	0.6	1.3565	1.0246	-0.707165
9	3.38762e+007	1145	0.55	0.614888	1.0264	-0.862227
10	3.33509e+007	38	0.55	0.674986	1.0246	-0.707167

Body: FLEX_BODY_1 — Radius: 0.0
Analysis: Last_Run — Threshold: 0
Criterion: Von Mises — File Format: HTML
Type: Stress — File Name:
Base Font Size: 10 — Report — Close

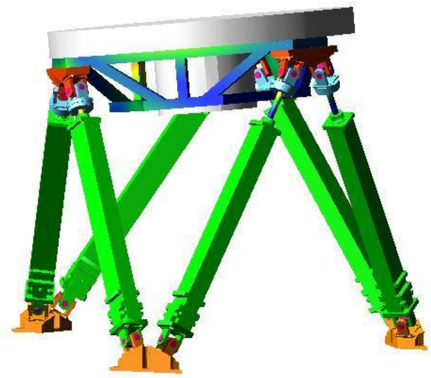

Figure 3.4 Von-Mises Stress values on the flexible top frame during testing simulation under 150 kg payload

The top frame is constructed from 6061 T6 aluminum alloy which has a yielding stress of 276 MPa. Maximum stress observed on the top frame is 42 MPa which is smaller than the yield stress value. So neither flexible shaft nor flexible top frame has been deformed plastically and the iterative analysis process should continue.

The density of the dummy weight is increased and the payload became 250 kg. When the stress values on the flexible shaft are observed on the hot spots table in Figure 3.5 the maximum stress value is seen as 104 MPa.

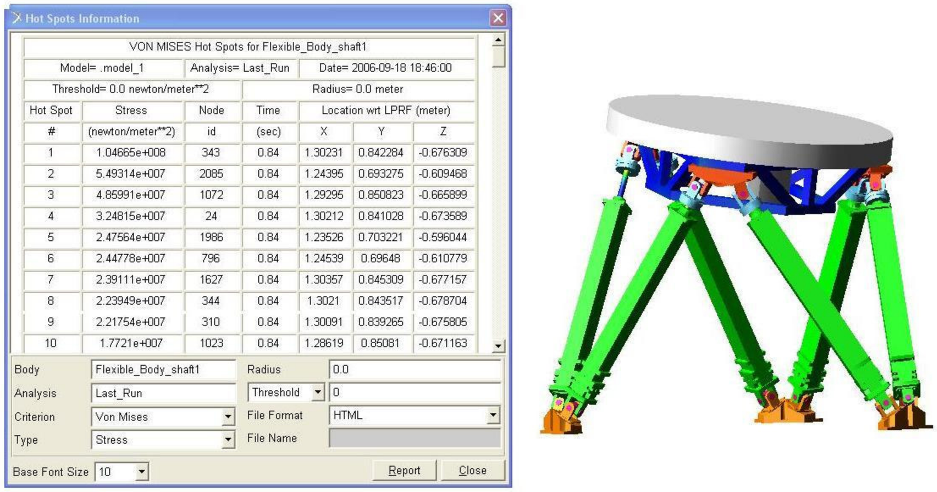

VON MISES Hot Spots for Flexible_Body_shaft1						
Model= .model_1	Analysis= Last_Run		Date= 2006-09-18 18:46:00			
Threshold= 0.0 newton/meter**2			Radius= 0.0 meter			
Hot Spot	Stress	Node	Time	Location wrt LPRF (meter)		
#	(newton/meter**2)	id	(sec)	X	Y	Z
1	1.04665e+008	343	0.84	1.30231	0.842284	-0.676309
2	5.49314e+007	2085	0.84	1.24395	0.693275	-0.609468
3	4.85991e+007	1072	0.84	1.29295	0.850823	-0.665899
4	3.24815e+007	24	0.84	1.30212	0.841028	-0.673589
5	2.47564e+007	1986	0.84	1.23526	0.703221	-0.596044
6	2.44778e+007	796	0.84	1.24539	0.69648	-0.610779
7	2.39111e+007	1627	0.84	1.30357	0.845309	-0.677157
8	2.23949e+007	344	0.84	1.3021	0.843517	-0.678704
9	2.21754e+007	310	0.84	1.30091	0.839265	-0.675805
10	1.7721e+007	1023	0.84	1.28619	0.85081	-0.671163

Figure 3.5 Von-Mises Stress values on the flexible shaft during testing simulation under 250 kg payload

The stress values on the top frame is shown in Figure 3.6.

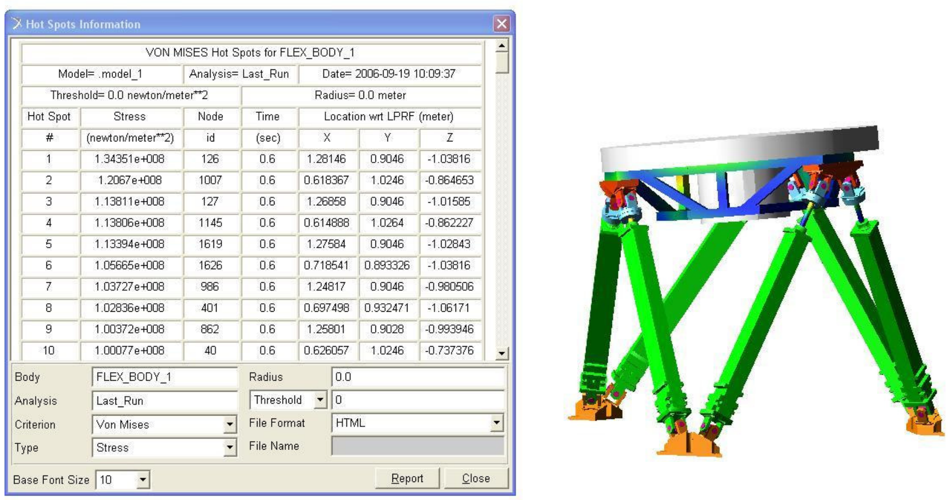

VON MISES Hot Spots for FLEX_BODY_1						
Model= .model_1	Analysis= Last_Run		Date= 2006-09-19 10:09:37			
Threshold= 0.0 newton/meter**2			Radius= 0.0 meter			
Hot Spot	Stress	Node	Time	Location wrt LPRF (meter)		
#	(newton/meter**2)	id	(sec)	X	Y	Z
1	1.34351e+008	126	0.6	1.28146	0.9046	-1.03816
2	1.2067e+008	1007	0.6	0.618367	1.0246	-0.864653
3	1.13811e+008	127	0.6	1.26858	0.9046	-1.01585
4	1.13806e+008	1145	0.6	0.614888	1.0264	-0.862227
5	1.13394e+008	1619	0.6	1.27584	0.9046	-1.02843
6	1.05665e+008	1626	0.6	0.718541	0.893326	-1.03816
7	1.03727e+008	986	0.6	1.24817	0.9046	-0.980506
8	1.02836e+008	401	0.6	0.697498	0.932471	-1.06171
9	1.00372e+008	862	0.6	1.25801	0.9028	-0.993946
10	1.00077e+008	40	0.6	0.626057	1.0246	-0.737376

Figure 3.6 Von-Mises Stress values on the flexible top frame during testing simulation under 250 kg payload

The maximum stress value on the flexible top frame under 250 kg payload during testing simulation is 134 MPa. The critical values are not reached for both of the critical parts so the dummy weight is increased to 400 kg and the results are observed once more. Figure 3.7 shows the results with 400 kg.

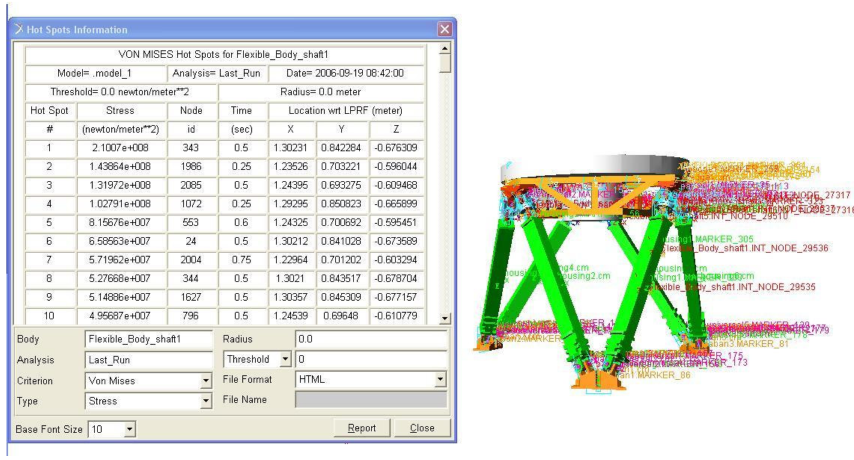

VON MISES Hot Spots for Flexible_Body_shaft1						
Model= .model_1		Analysis= Last_Run		Date= 2006-09-19 08:42:00		
Threshold= 0.0 newton/meter**2			Radius= 0.0 meter			
Hot Spot	Stress	Node	Time	Location wrt LPRF (meter)		
#	(newton/meter**2)	id	(sec)	X	Y	Z
1	2.1007e+008	343	0.5	1.30231	0.842284	-0.676309
2	1.43864e+008	1986	0.25	1.23526	0.703221	-0.596044
3	1.31972e+008	2085	0.5	1.24395	0.693275	-0.609468
4	1.02791e+008	1072	0.25	1.29295	0.850823	-0.665899
5	8.15676e+007	553	0.6	1.24325	0.700692	-0.595451
6	6.58563e+007	24	0.5	1.30212	0.841028	-0.673589
7	5.71962e+007	2004	0.75	1.22964	0.701202	-0.603294
8	5.27668e+007	344	0.5	1.3021	0.843517	-0.678704
9	5.14886e+007	1627	0.5	1.30357	0.845309	-0.677157
10	4.95687e+007	796	0.5	1.24539	0.69648	-0.610779

Figure 3.7 Von-Mises Stress values on the flexible shaft during testing simulation under 400 kg payload

The maximum stress value on the flexible shaft is increased to 210 MPa whereas the stress values of the top frame is shown in Figure 3.8.

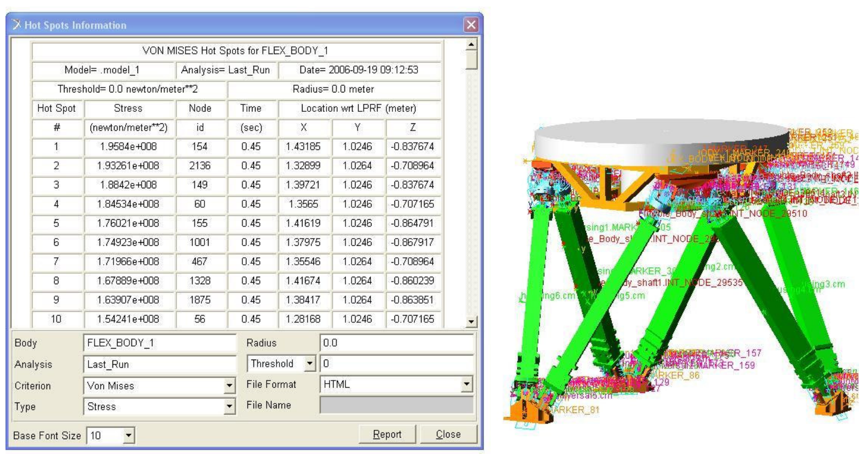

VON MISES Hot Spots for FLEX_BODY_1						
Model= .model_1		Analysis= Last_Run		Date= 2006-09-19 09:12:53		
Threshold= 0.0 newton/meter**2			Radius= 0.0 meter			
Hot Spot	Stress	Node	Time	Location wrt LPRF (meter)		
#	(newton/meter**2)	id	(sec)	X	Y	Z
1	1.9584e+008	154	0.45	1.43185	1.0246	-0.837674
2	1.93261e+008	2136	0.45	1.32899	1.0264	-0.708964
3	1.8842e+008	149	0.45	1.39721	1.0246	-0.837674
4	1.84534e+008	60	0.45	1.3565	1.0246	-0.707165
5	1.76021e+008	155	0.45	1.41619	1.0246	-0.864791
6	1.74923e+008	1001	0.45	1.37975	1.0246	-0.867917
7	1.71966e+008	467	0.45	1.35546	1.0264	-0.708964
8	1.67889e+008	1328	0.45	1.41674	1.0264	-0.860239
9	1.63907e+008	1875	0.45	1.38417	1.0264	-0.863851
10	1.54241e+008	56	0.45	1.28168	1.0246	-0.707165

Figure 3.8 Von-Mises Stress values on the flexible top frame during testing simulation under 400 kg payload

The maximum stress value on the flexible top frame is increased to 195 MPa. The iteration should continue. The payload is increased to 600 kg with the results shown in Figure 3.9.

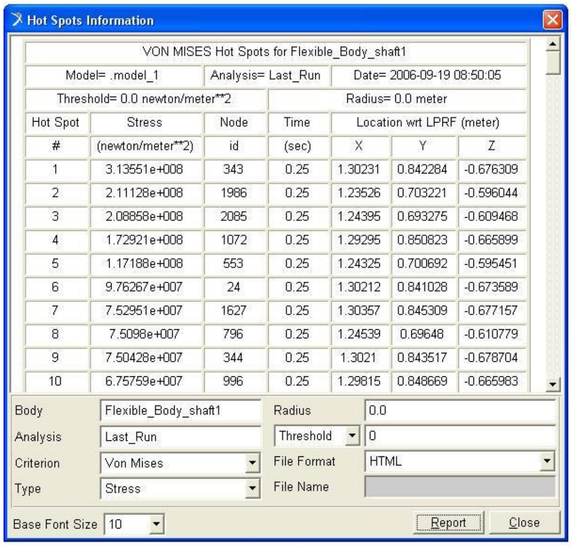

Hot Spot #	Stress (newton/meter**2)	Node id	Time (sec)	Location wrt LPRF (meter) X	Y	Z
1	3.13551e+008	343	0.25	1.30231	0.842284	-0.676309
2	2.11128e+008	1986	0.25	1.23526	0.703221	-0.596044
3	2.08858e+008	2085	0.25	1.24395	0.693275	-0.609468
4	1.72921e+008	1072	0.25	1.29295	0.850823	-0.665899
5	1.17188e+008	553	0.25	1.24325	0.700692	-0.595451
6	9.76267e+007	24	0.25	1.30212	0.841028	-0.673589
7	7.52951e+007	1627	0.25	1.30357	0.845309	-0.677157
8	7.5098e+007	796	0.25	1.24539	0.69648	-0.610779
9	7.50428e+007	344	0.25	1.3021	0.843517	-0.678704
10	6.75759e+007	996	0.25	1.29815	0.848669	-0.665983

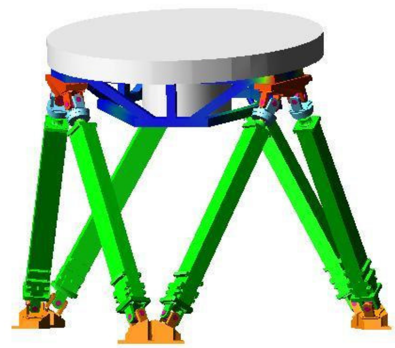

Figure 3.9 Von-Mises Stress values on the flexible shaft during testing simulation under 600 kg payload

The maximum stress value on the flexible shaft is 313 MPa which is greater than the critical value of the steel that is 215 MPa. The iteration should be finalized since the shaft deforms plastically at this payload value. So the maximum payload that the platform should carry without any mechanical unwanted deformation is 600 kg. If the stress values are observed on the flexible top frame at this payload it can be seen that the maximum stress is 342 MPa which is greater than the critical value of aluminum that is 276 MPa.

CHAPTER 4

DISCUSSION AND CONCLUSIONS

4.1 Summary and Conclusions

This thesis is focused on solid modeling, modal testing, virtual dynamic analyzing and construction of a Stewart Platform. ASELSAN requires a six degree of freedom motion simulator which should simulate dynamic motions of the tank on APG track in terms of rotational velocities and linear accelerations. In order to fulfill this requirement, a Stewart Platform is designed and constructed. Solid modeling, modal testing and virtual dynamic simulation are the important steps of this work; and they are discussed in detail throughout the study.

In this thesis, ProEngineer Wildfire® is used for solid modeling the components, the sub-assemblies and the final assembly, ANSYS Workbench® is used for investigating the modal behavior of the components, ADAMS® 2003 is used for the dynamic simulation of the mechanism, ADAMS/Flex®, ADAMS/AutoFlex® and ADAMS/Durability® are used to analyze the results when flexibility is embedded into the system.

In stabilized head mirror tests, this Stewart Platform has been widely used not only in control system design of the head mirror but also structural dynamics testing of it. The Stewart Platform enables the design engineers to see the shortcomings of their design and observe the problems in their prototypes in advance and in laboratory conditions. In this aspect, the efficient utilization of the Stewart Platform decreases development period of the head mirror and reduces the associated development cost significantly.

The construction of the platform is performed and the system components are manufactured. In order to do manufacturing technical drawings are prepared with required geometrical and dimensional tolerances. Different manufacturing processes are used up to the extent in order to prepare perfect housings and adapters for the critical components. Five technical drawings without tolerances and with nominal dimensions are given in the Appendix in order to give an intuition about the manufacturing period. These drawings include the front, side, top views of the full Stewart Platform assembly. The other two drawings are the top frame and the base. The outline dimensions and the wireframe appearances of the components can prescribe the system briefly. Lastly an image of the Stewart Platform is given in ASELSAN facilities during operation. The platform is shown with the testing equipment and with the sensors mounted on it.

4.2 Future Scope

The CAD software can be used with user-defined macros. In this thesis these software is used in an iterative approach since it is critical to see what happens at the end of each iteration. But once the intuition of "What Happens?" is gathered the design parameters can be read into the system once and the process may continue until the design values are matched.

When investigating the maximum payload that the platform can handle, the testing simulation used is the trajectory that the platform is used during stabilized head mirror tests. This trajectory may be standardized in order to benchmark different designs.

REFERENCES

1 Gürcan, B., Balkan, T., Başçuhadar, İ. *Stabilization of a two axis hydraulic motion simulator,* MTM, MST, ASELSAN, 2001

2 Söylemez, E., *Mechanisms,* METU, 1999

3 Karayumak, T., *Design and Manufacturing of a two degree of freedom gyro stabilized opto-mechanical platform, A Master Thesis,* Mechanical Engineering Department, METU, 2003

4 Gürbüz, S., *Using of ADAMS/View® software during the mechatronic design period of a six axis motion simulator,* MSC. Software User's Conference, İstanbul, 2006

5 Gürbüz, S., *Six axis motion simulator,* ASELSAN Journal Vol.2, pp.31-33, Ankara, 2006

6 EXLAR Inc., *Exlar Product Catalogue,* URL: http://www.exlar.com, Last occurred November 2006

7 BELDEN Inc., *Belden Product Catalogue,* URL: http://www.beldenuniversal.com, Last occurred November 2006

8 CURTIS Universal Joint Company Inc., *Curtis Universal Product Catalogue,* URL: http://www.curtisuniversal.com, Last occurred November 2006

9 PARKER Inc., *Parker Linear Actuator Product Catalogue,* URL: http://www.parker.com, Last occurred November 2006

10 RACO Inc., *Raco Linear Actuator Product Catalogue,*
URL: http://www.raco.de, Last occurred November 2006

11 MSC. Software Corporation, *MSC. ADAMS Basic Full Simulation Training Guide,* Version 1.0, 2001

12 MSC., Software Corporation, *Getting started using ADAMS/AutoFlex*®, Version 1.0, 2003

13 Özdağlar, M., *Dynamic Modeling and Control of a Stewart Platform type motion simulator, A Master thesis,* Mechanical Engineering Department, METU, 2001

14 Albayrak, O., *Modeling and Real-Time Control System Implementation for a Stewart Plaform, A Master Thesis,* Mechanical Engineering Department, METU, 2006

APPENDIX

A. Technical Drawings with nominal dimensions

A.1 Front View of the assembly

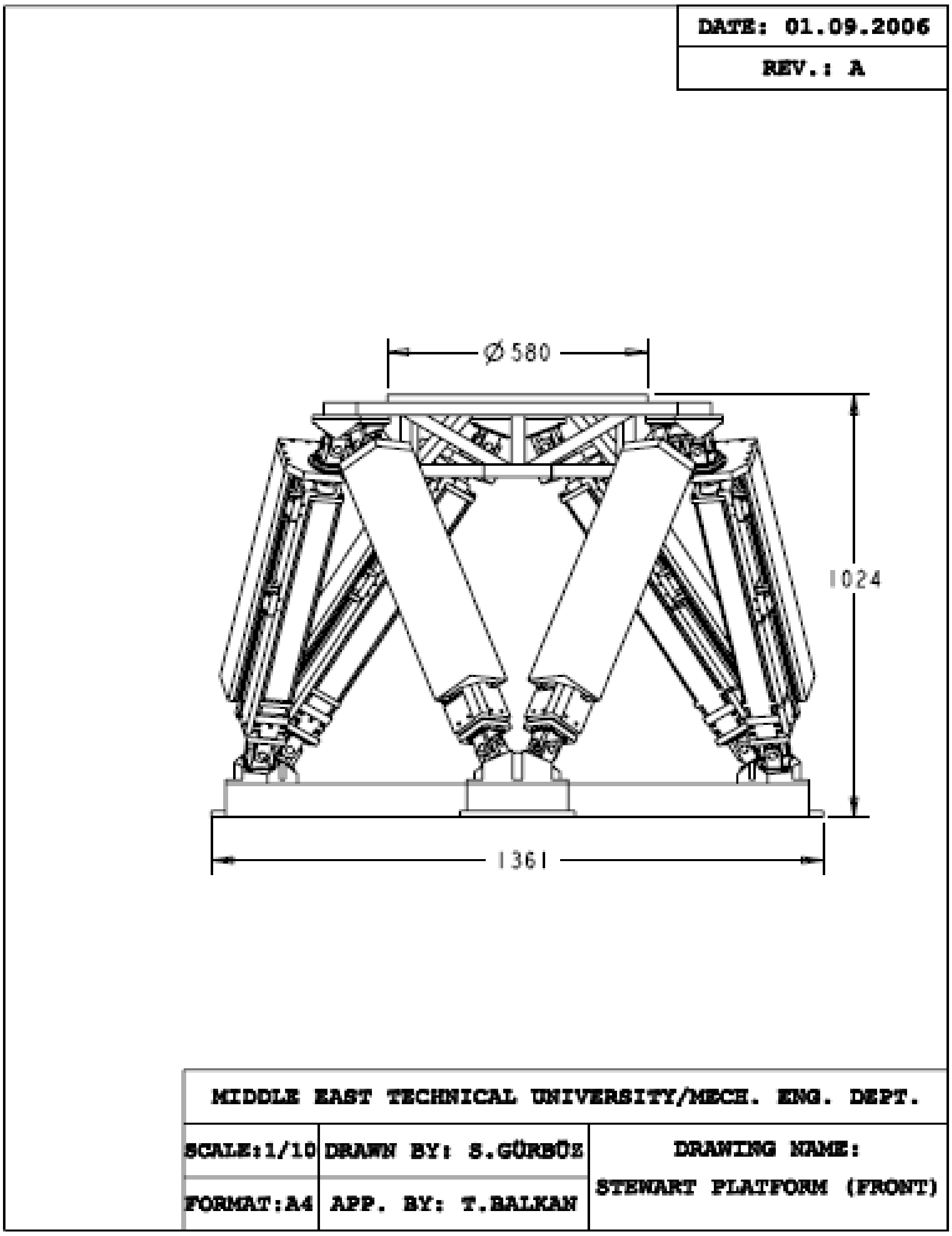

Figure A.1 Technical Drawing of the Front View of the assembly

A.2 Side View of the assembly

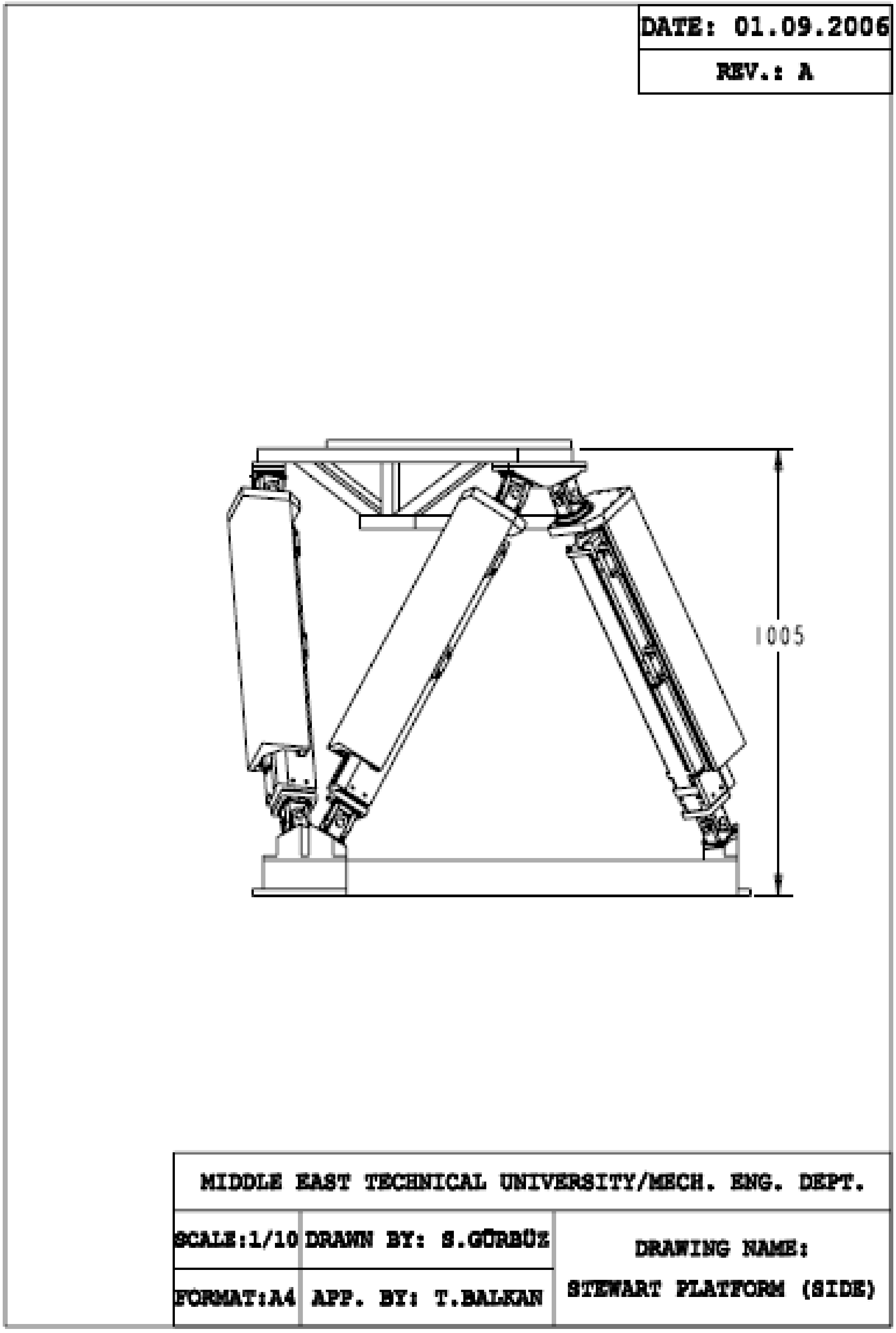

Figure A.2 Technical Draing of the Side View of the assembly

A.3 Top view of the asssembly

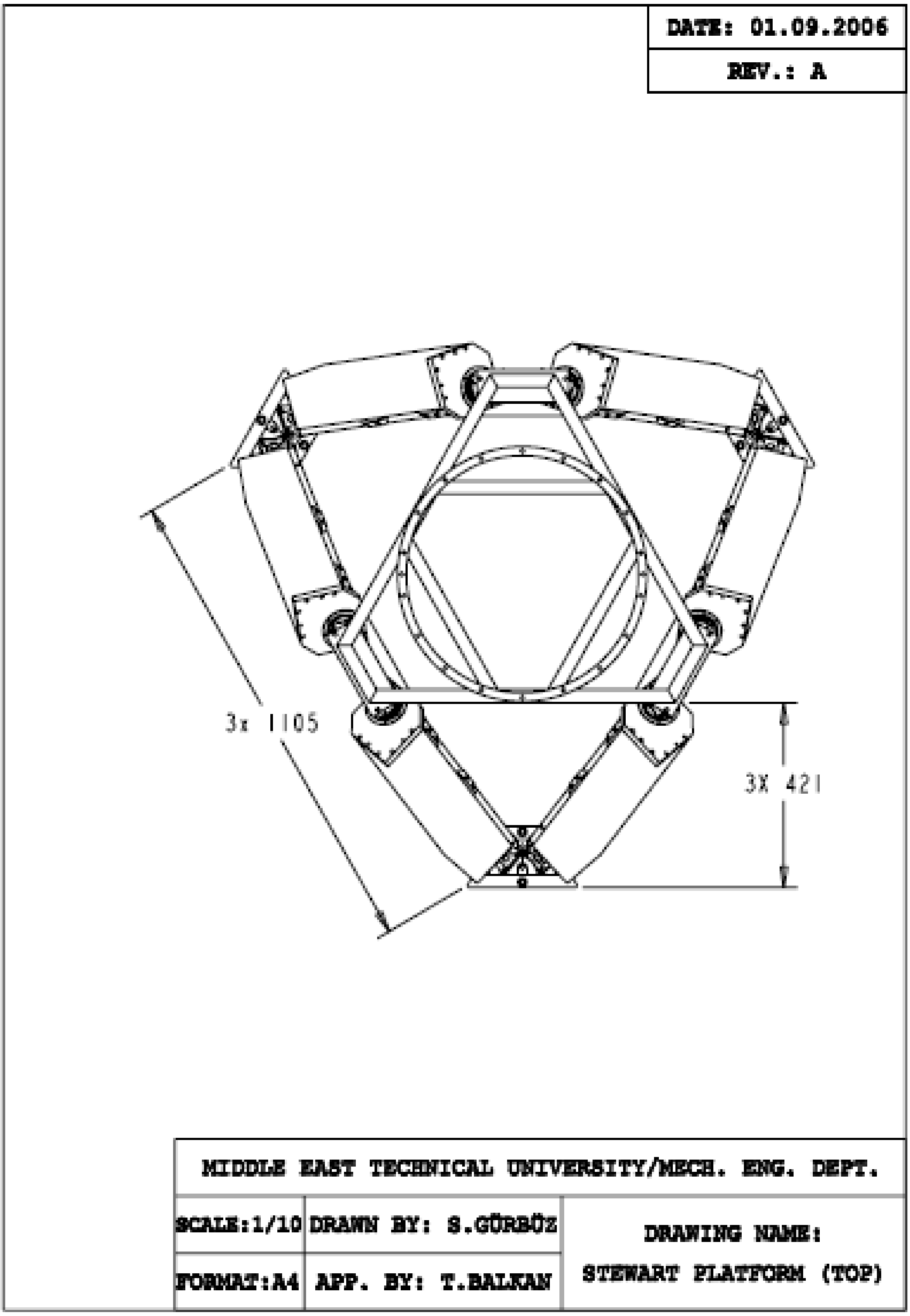

Figure A.3 Technical Drawing of the Top View of the assembly

A.4 Top Frame

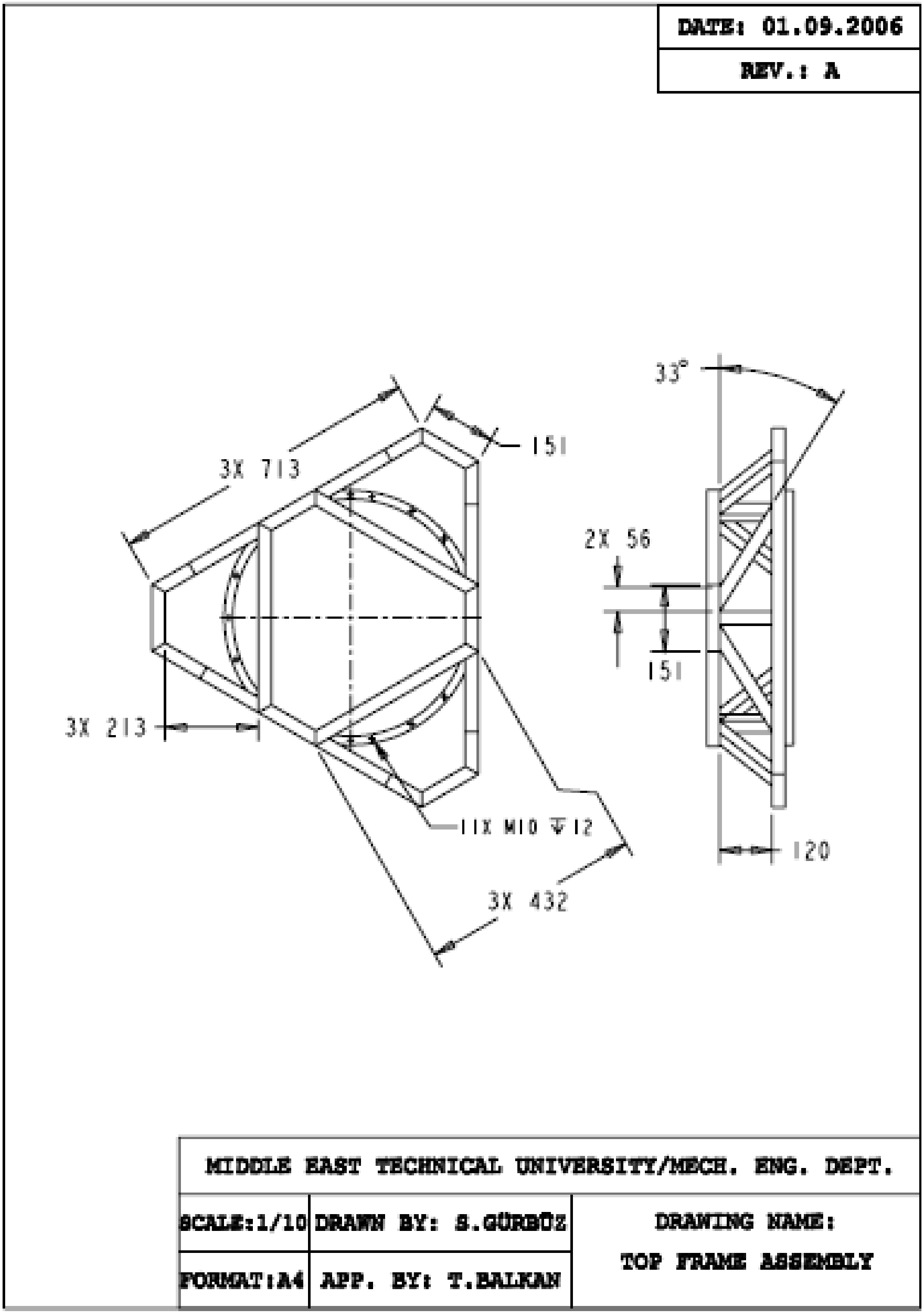

Figure A.4 Technical Drawing of the Top Frame

A.5 The Base

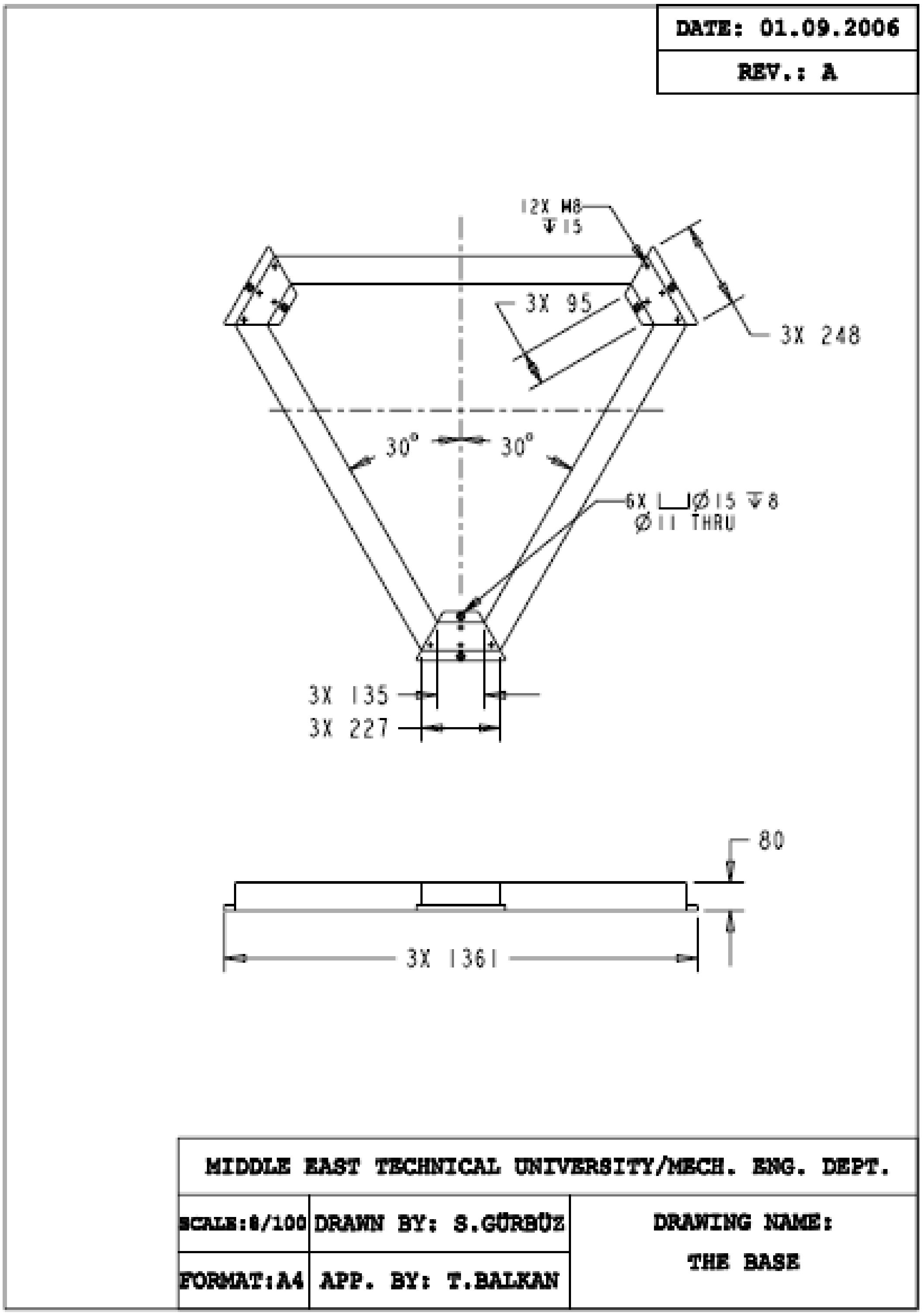

Figure A.5 Technical Drawing of the Base

B. An image showing Stewart Platform during operation

Figure B.1 Stewart Platform